MORTEN ROSLAND
SUPERVISOR: ARILD SAASEN
EXTERNAL SUPERVISOR: KARL RONNY KLUNGTVEDT

The Rheological Impact of Polymers and Salt on Xanthan Gum in Drilling Fluids

Bachelor thesis 2024
Energy and Petroleum technology
Faculty of Science and Technology
Department of energy and Petroleum Engineering

University of Stavanger

Acknowledgement

Abstract

Drilling fluids serve a vital role during drilling operations. They are divided into water based muds (WBM) and oil based muds, the choice between them depends on specific project needs. Xanthan gum is a highly popular WBM additive due to its high viscosity at low concentrations. It also has a good salt tolerance and exhibits the desirable pseudoplastic behavior of a drilling fluid.

This thesis presents a study that investigates how xanthan gum is affected by polymers and salts. Using an aqueous xanthan gum base, 16 samples were prepared. By adding various combinations of polymers and salts, the rheology of the fluids was tested.

Shear stress measurements using a viscometer are conducted. Hot rolling to simulate mechanical and thermal wear is done. The linear viscoelastic region of selected samples is analyzed using a rheometer. Additionally, measurements using zeta potential apparatus are performed.

The results show that salts improve the fluids stability and decreases the yield stress. However, $CaCl_2$ seemed to have a degradable effect on the fluid when using a cellulose based polymer. The study finds indications that starch based polymers bond better with xanthan gum compared to cellulose based polymers.

List of Contents

Nomenclature

Greek symbols

$\dot{\gamma}$ – Shear rate

θ – Deflection

τ – Shear stress

τ_f – Flow point

τ_s – Surplus stress

τ_y – Yield stress

Abbreviations

AHR – After Hot-Rolling

API – American Petroleum institute

AS – Amplitude sweep

BHR – Before Hot-Rolling

CMC – Carboxy Methyl Cellulose

CSD – Controlled Shear Deformation

CSS – Controlled Shear Stress

DLS – Dynamic Light Scattering

G' – Storage Modulus

G" – Loss Modulus

HPHT – High Pressure High Temperature

K – Consistency Factor

LVE – Linear Viscoelastic

n – Shear thinning index

OFITE – OFI testing equipment

PAC – Poly Anionic Cellulose

RPM – Revolutions Per Minute

SG – Specific Gravity

WBM – Water Based Mud

XC – Xanthan Gum

List of Tables

List of Figures

1 Introduction

When drilling a well, a drilling fluid serves a vital role in optimizing performance. Some of its important functions is to provide sufficient colling of the drill bit, transport of cuttings. ensuring pressure stability and a proper lubrication of the drill string. A typical water-based mud (WBM) consists of various components to ensure the mentioned parameter functions are fulfilled. The buildup of a WBM consists of water, some type of salt, weight materials, viscosifying polymers and fluid loss materials. All these components have an impact on the fluid's rheology. The book Fundamentals of Sustainable Drilling Engineering by Hossain & Al-Majed (2015) further describes the build up and the function of drilling fluids in chapter 3. The polymers main task is to control the viscosity and providing stable fluids at a high variety of temperatures and pressures. Recently, the focus of implementing polymers has shifted from a stability focus to improving its performance in harsh conditions such as high-pressure and high-temperature (HPHT) and high salt concentrations (Davoodi et al., 2024).

Some of the most accessible modified natural polymers include starch, xanthan gum (XC), guar gum and different types of cellulose agents such as carboxy-methyl-cellulose (CMC) and poly-anionic-cellulose (PAC) (Davoodi et al., 2024). Polymer fluids exhibit a pseudoplastic behavior, also known as shear thinning. Meaning their viscosity decrerases at higher shear rates. The base for all the fluids tested, is xanthan gum. A highly versatile additive used in WBMs to control the viscosity of the fluid. Xanthan gum has several important properties making it useful in drilling applications (Chaturvedi et al., 2021). Such as a high viscosity at low concentrations stable within the pH range of 2-12 and good thermostability. It is pseudoplastic wich improves cuttings transport in the annulus. XC also has a high solubility, good thermostability and a high salt tolerance. XC also displays good properties in terms of reducing the formation permeability (Klungtvedt & Saasen, 2022b)

A common model for describing pseudoplastic fluids with a yield stress is the Herschel-Bulkley model in Equation 1.1. This model expresses a relationship between the following parameters: shear stress (τ), shear rate ($\dot{\gamma}$), yield stress (τ_y), the power-law index (n), and the consistency factor (K). In this equation the index n and factor K depend on each other meaning they cannot be considered as a standalone fluid property (Saasen & Ytrehus, 2020). Therefore, two different approaches have been made to better describe the consistency index.

$$\tau = \tau_y + K\dot{\gamma}^n \qquad \qquad 1.1$$

Firstly Nelson & Ewoldt (2017) introduced a characteristic shear rate of the fluid. Where $\dot{\gamma}_c$ is the shear rate where $\tau = 2*\tau_y$. Due to its limitations regarding typical properties of drilling fluids such as low yield strength. Saasen & Ytrehus (2020) introduced a modified model with dimensionless shear rates and a surplus stress (τ_s) as shown in Equation 1.2. The definition of the surplus stress is shown in Equation 1.3. Another benefit of τ_s is that it does not depend on the curvature index and can therefore be used as a fixed property of the fluid. The yield stress and is calculated using Equation 1.4 as described by Power and Zamora (2003). The shear thinning index is calculated using Equation 1.5. Where θ is the reading at the given shear rate in 1/s. The viscosity (η) of a fluid is directly related with shear stress values and is calculated using Equation 1.6.

$$\tau = \tau_y + \tau_s \left(\frac{\dot{\gamma}}{\dot{\gamma}_s}\right)^n \qquad\qquad 1.2$$

$$\tau_s = \tau - \tau_y \qquad\qquad 1.3$$

$$\tau_y = 2 * \theta_{10.22} - \theta_{5.11} \qquad\qquad 1.4$$

$$n = \frac{\ln(\theta_{1022} - \tau_y) - \ln \tau_s}{\ln(102.2 - 1.7023)} \qquad\qquad 1.5$$

$$\eta = \frac{\tau}{\dot{\gamma}} \qquad\qquad 1.6$$

The scope of the presented material is to investigate key differences of other polymers and salts effect on xanthan gum. Another aspect is the impact from different salts, such as type and concentration. Used polymers are Poly-Anionic Cellulose (PAC) and two types of starch: Ndril-HT plus and Dextrid E.

Experimental methods encompass:

- Concentric cylinder measurements, to describe shear stress as a function of shear rate.
- Hot rolling to investigate thermal and mechanical wear.
- Oscillary tests using a rheometer, to study the fluids viscoelastic properties.
- Zeta-potential measurements, to access the applicability of zeta-potential theory to polymers.

2 Theoretical background

2.1 Polymer Chemistry

Xanthan gum is a biodegradable polymer related to cellulose and starch polymers, its backbone consists of a variant of the cellulose molecule (Mateus & Rosângela, 2019). Additionally, acetate and pyruvate groups are attached to the cellulose structure as in Figure 2.1.1.
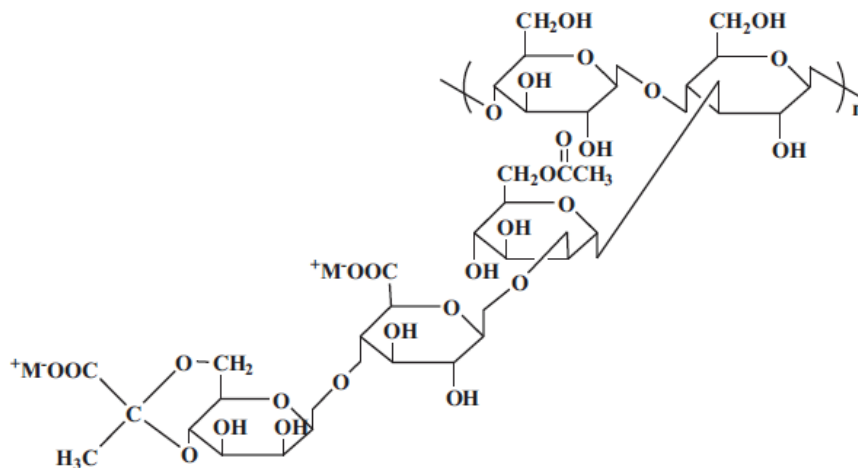
Figure 2.1.1: Chemical structure of XC (Mateus & Rosângela, 2019).

PAC, Ndril HT and Dextrid E are all polymers composed of repeated glucose monomers. What separates them is the orientation of the molecules as shown in Figure 2.1.2. Cellulose consists of linked monomers. Each glucose units rotates 180 degrees while the glucose units in starch have the same orientation. Additionally, cellulose tends to consist of much longer chains of glucose, which might lead to higher viscosity.
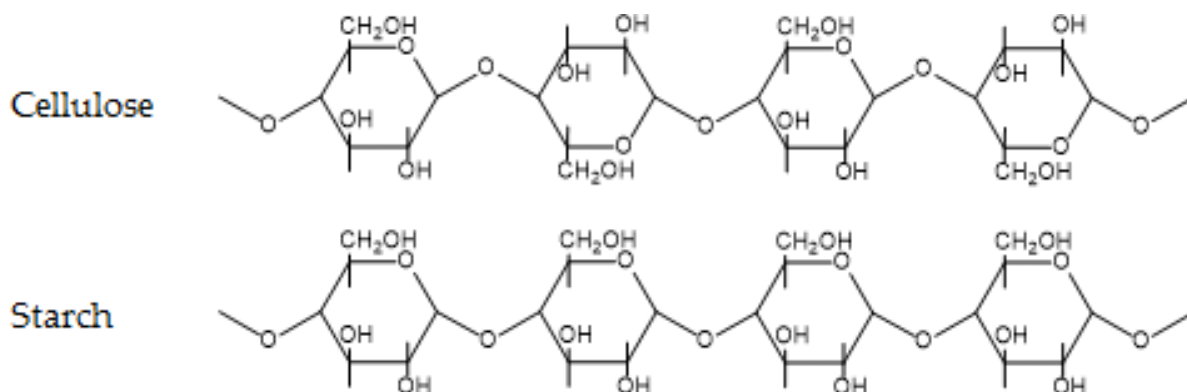
Figure 2.1.2: Chemical structure of cellulose and starch (Nakajima, Dijkstra, & Loos, 2017).

Ndril HT and Dextrid E are starch based polymers, but they differ in the components. The Dextrid E is listed with complex carbohydrate as its main substance, Ndril is listed with modified starch as its main substance. More info on the substances concentration and components are withheld as proprietary by the manufacturer Halliburton.

The diffferent additives have different purposes in a drilling fluid. Starch is in addition to a viscosity controller, also a material used to control the fluid loss. The fluid loss is desirable to keep at a minimum to avoid leakage to the formation when drilling. Crosslinked starch such as

Ndril HT has shown and effective increase in gel strenght. It seems that increased degree of crosslinking of a polymer shows higher increase in yield strenght (Wei et al., 2023). PAC on the other hand consists of longer cellulose chains increasing the viscosity more than starch. Busch et al., (2018) tested aqueous PAC solutions and found that the solutions did not have a yield stress as G'' where constantly larger than G'. The absence of yield stress was also confirmed using simpler models on a fann viscometer. The properties G' and G'' is further described in chapther 2.3.

2.2   Salt Effect on Polymers

Salt dissolved in water will form a solution consisting of positive and negative ions. For example, sodium chloride dissolved in water will form the ions Na^+ and Cl^- as shown in Equation 3.1:

$$NaCl(s) \overset{H_2O(l)}{\rightleftharpoons} Na^+(aq) + Cl^-(aq)$$

<div align="right">2.1</div>
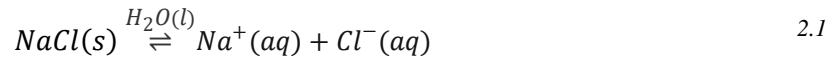
Poly-anionic cellulose (PAC) is anionic, meaning the particle surface has a negative charge and thus attracting positive charges. When dissolved in salt water, the positive charged ions will form a bond with the polymers. The bond will cause the PAC to change its behavior and as a result, increase its conductivity. As for the example of NaCl above, monovalent Na^+ ions will form. Using salt such as calcium chloride ($CaCl_2$), divalent Ca^{2+} ions will form. The presence of divalent ions can form two bonds with the polymers in the fluid. Whilst monovalent ions can only form one bond

Solutions involving salts and xanthan gum studies have produced contradictory results. Mateus & Rosângela (2019) discusses that increasing salt initially decreases viscosity, followed by a turning point where viscosity increases. Some find only a slight increase in viscosity for diluted xanthan gum solutions with sodium chloride. Others, claims that the viscosity of the solution decreases more moderately. XC solutions forms a gel substance. Mohammed et al. (2007) studied the effect of calcium ions on XC solutions and found that Ca^{2+} ions increase the gel-like behavior at small concentrations. It has a turning point where the gel-like properties sharply reduce. Another study done by Nsengiyumva et al. (2023) found that salt have a bigger effect than temperature on aqueos xanthan gum solution. Na^+ salts compacts the XC structure. For Ca^{2+}, this effect was even more significant. It was also found that increased temperature expands the structure. The viscosity of xanthan gum increases because of a larger coil structure at increasing temperatures. As a result, salts reduces the effect of higher temperatures on the xanthan gum.

An important aspect to keep in mind is the chemistry of the water molecule (H_2O), which is a polar covalent molecule. Where hydrogen atoms are positive, and the oxygen atoms are negative. In a solution containing anionic polymers and salt ions, hydrogen atoms will also form bonds with the negative charged polymer. Salts with a higher positive charge will then outcompete the hydrogen atoms. Thus, being more likely to form a bond with the anionic polymers.

2.3 Amplitude Sweeps

More advanced tests using a rheometer are being used to analyze drilling fluids (Ofei et al., 2023; Busch et al., 2018). Amplitude sweeps will give a more accurate view of the fluids properties at low shear rates in the linear viscoelastic (LVE) region. Viscosity measurements using a concentric viscometer is less accurate at lower shear rates (Allouche et al., 2014). To get a better understanding of the fluid's LVE region. Oscillation tests can be done to get a more accurate view of the fluids yield stress, flow point (τ_f), storage modulus (G') and loss modulus (G''). The samples are viscoelastic meaning G' > G''. The fluid can be considered a "soft-solid" at shear stresses under the yield point (Mezger, 2015). The flow point is the value where G' intersects G''. The yield point "is the value of the shear stress at the limit of the LVE region" (Anton Paar, 2024).

To preset the deflection, two modes are available. A shear strain-amplitude-sweep with a controlled shear deformation (CSD) and shear-stress-amplitude sweep with a controlled shear stress (CSS) (Mezger, 2015). The selected method for analysis is the shear-stress-amplitude sweep with CSS because this will provide a good visual presentation of the relevant data. Another benefit is that the units on the x and y axis uses stress in Pa. Which is more easily relatable compared to the applied strain in percent.

2.4 Zeta Potential

When particles are dispersed in a liquid, a counter charge develops at the slipping plane of the molecule, this can be measured and is called the Zeta potential (Shashikant et al., 2022). The different polymers and additives presented in this thesis are particles with a charged surface. XC are anionic, meaning a negative charge will develop and thus attract other positive charged particles. There are three main factors affecting the zeta potential: pH value, conductivity, and the concentration of a formulation component. In general, the zeta potential is positive at a low pH and negative for high pH values. For the used samples the salt is the main contributor to conductivity. the effect of increased amount of salt in a buffer will decrease the zeta potential (Nobbmann, 2018).

3 Methodology

This chapter the experimental methods used to investigate the properties of the tested fluids is outlined. It also provides a brief introduction to the key equipment employed. A complete list of all the equipment used is attached in Appendix B and a simplified illustration of the procedure is attached in Appendix F.

3.1 Sample Preparation

The recipes are designed to have a volume of 350 mL, making it practical to convert units between the SI-system and US-field units. As an example, 1-gram component per 350 mL is the equivalent of 1 lbs/bbl. Each sample fluid is mixed using a Hamilton Beach mixer following the order of the recipes listed in Appendix A. Mettler Toledo weight and the mixer is shown in Figure 3.1.1. The amount of XC is always 1.5 g and the amount of a given polymers is always 5 g per sample. When any of these additives is discussed, the mentioned amounts are common for the used recipes. The amount will therefore not be mentioned further when referring to each sample. After each component is added to the fluid in the given order, the mixer is set at full speed for 10 minutes. Table 3.1 shows the components used. The correct amount of salt and water is calculated using the python code from Appendix G and salt tables from AMC Drilling Optimisation (2019). Thus, ensuring that each sample always equals 350 mL.

Table 3.1: Components used in this thesis.

Component [Chemical formula]	Description/function
Water [H_2O]	Solvent
Soda ash [Na_2CO_3]	Controlling alkalinity
Caustic Soda [NaOH]	Controlling alkalinity
Barazan D, Xanthan Gum (XC)	Increasing viscosity
Magnesium oxide [MgO]	Controlling alkalinity
Sodium chloride [NaCl]	Salt used to study effect on fluid
Calcium chloride [$CaCl_2$]	Salt used to study effect on fluid
Potassium sulfate [K_2SO_4]	Salt used to study effect on fluid
N-DRIL HT PLUS	Starch based polymer
Dextrid E	Starch based polymer
Poly-anionic cellulose, PAC-L	Cellulose based polymer
Auracoat UF	Cellulose based agent

After mixing, the fluids viscosity measurements are conducted. Thereafter, the fluid is put in the Ofite roller oven displayed in Figure 3.1.1 at a temperature of 90° C for 16 hours. The hot rolling is conducted using two parallels. Where one of the cells is added threaded steal rod as in Figure 3.1.2 to simulate mechanical wear. This method of simulating realistic well conditions were published by Klungtvedt & Saasen (2022a).

When mixing the xanthan gum and the added polymers, bubbles were formed. Due to a high viscosity these bubbles are tricky to eliminate and will affect the accuracy of the readings. Attempts using a vacuum chamber and a centrifuge to eliminate them were conducted without success. After hot rolling (AHR) at 90° C, the bubbles were eliminated due to the high temperature. It is therefore decided to not mix the fluid with a high rpm mixer AHR. Instead,

the fluid is mixed gently by hand to avoid the bubbles and gently distribute the particles in the fluid. In addition, there are no weight materials present in most of the recipes, reducing the presence of sag particles in the fluid.

Figure 3.1.1: Ofite roller-oven (left), Hamilton Beach mixer (middle), Mettler Toledo PB1502-S/FACT (right).

Figure 3.1.2: Threaded steel rods.

3.2   Viscosity measurements

Viscosity and shear stress properties are measured using a concentric cylinder viscometer satisfying API requirement. The two cylinders in the apparatus has the following functions:

Concentric cylinders:
- The rotor (outer) is spun at a constant shear rate, thus causing the fluid in the annular space to apply a torque to the bob.
- The bob (inner) is suspended by a torsion spring measuring force. The movement of the bob can then be read at the top of the device.

Viscometer measurements are conducted before and after Hot-Rolling. The measurements is performed using the viscometer shown in Figure 3.2.1 at the following shear rates in RPM: 600, 300, 200, 100, 60, 30, 6 and 3, corresponding to the following shear rates in 1/s: 1022, 511, 341, 170, 102, 51.1, 10.2 and 5.1.

Figure 3.2.1:Viscometer-Ofite Model 800 8-speed.

3.3   Measuring zeta-potential

The measurement of the zeta potential is conducted using the Malvern Zetasizer Advanced series shown in Figure 3.3.1. The measurement is carried out using dynamic light scattering (DLS). In which you have a sample cell containing two electrodes, a single frequency laser and a detector. The detector measures the speed of electrons moving towards the electrodes. The device can then transfer this data to the obtained measured Zeta potential in millivolts. Part of the challenges measuring zeta-potential with DLS is that it is based on Brownian motion: the random movement of particles (Shashikant, et al., 2022). Polymers suspended in a liquid form some sort of structure, so that it is not fully Brownian motion. The tests are performed to verify if any of the theory can also be applied for the fluids in this thesis.
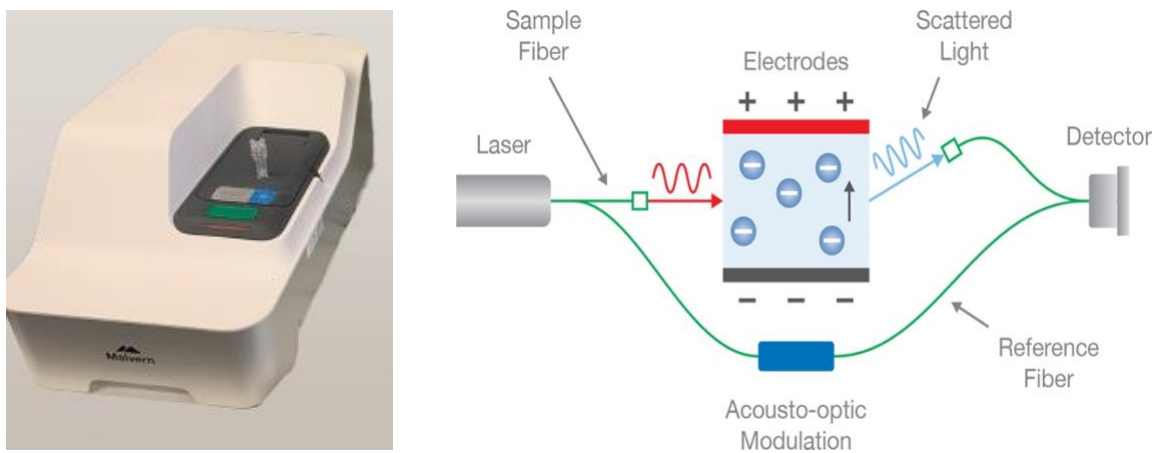
Figure 3.3.1: Malvern zetasizer (left). Measurement illustration (right) (Wyatt Technology, 2024)

3.4   Oscillation tests

Flow curve measurements and amplitude sweeps have been performed using the Anton Paar MCR 302 rheometer shown in figure shown in Figure 3.4.1. A rheometer has a broader range of capabilities compared to a concentric cylinder viscometer made in accordance with API. It provides a more accurate control of shear rates, shear stress and temperatures. It is also powerful in the context of measuring yield stresses using oscillary measurements. The further approach is described below in the given order.

- Amplitude sweeps: the cup is filled with the fluid being tested. The test is then started using a recovery time of 1 minute. The device then records 27 measurement points ranging from a shear oscillary strain of 0.01% to 300%.
- Flow curve: shear stress measurements are conducted at shear rates from 1000 to 0.1 1/s from highest to lowest. The initial measurement time is 3 s for highest shear rate to 120 s for the lowest shear rates. The device records 21 measurement points.

The procedure is performed at two different temperatures. One at 20 °C and one at 49 °C, as the general room temperature for viscometer measurements were around 20 °C. 49 °C is a more relevant temperature for testing and is used as the standard API temperature.
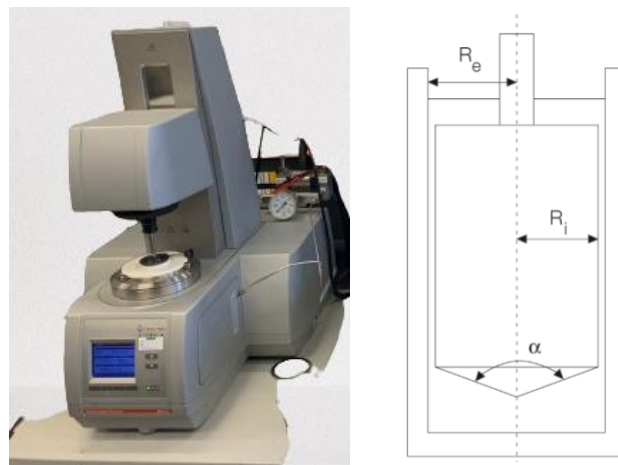
Figure 3.4.1: Anton Paar MCR 302 Rheometer (left). Illustration of the measurement chamber (right)

4 Experimental Work, Results and Discussion

In this chapter, the experimental work is presented in six sections:

- Flow curves and from the different samples BHR.
- Effects of mechanical and thermal wear AHR.
- Tests conducted with the rheometer to investigate the fluids properties in the LVE region.
- Flow curves from the more accurate rheometer.
- An analysis of the Herschel-Bulkley parameters and further discussing the effects of salt.
- Zeta potential measurements offering initial insight into the interactions between polymers and salt within the fluids.

Table 4.1 shows an overview of the discussed samples. When discussing these, they will be referred to as either its sample number or a simplified description of the fluid.

Table 4.1: Overview of the discussed samples in the thesis.

Sample number (from Appendix A)	If not referred to as sample number, it is referred to as:
1	XC
2	XC + PAC
3	XC + PAC + 50 g NaCl
4	XC + Ndril
5	XC + Ndril + 50 g NaCl
6	XC + Dextrid
7	XC + Dextrid + 50 g NaCl
8	XC + Ndril + Auracoat
9	XC + Dextrid + 25 g NaCl
10	XC + Ndril + 25 g NaCl
11	XC + PAC + 50 g $CaCl_2$
12	XC + PAC + 35 g K_2SO_4
13	XC + Ndril + 25 g $CaCl_2$
14	XC + Ndril + 25 g K_2SO_4
15	XC + Ndril + 50 $CaCl_2$
16	XC + Ndril + 100 g $CaCl_2$

4.1   Flow Curves Using Concentric Cylinder Viscometer

Figure 4.1.1 shows the measured shear stress values for XC solutions with 5 g of added polymers. The obtained modified Herschel-Bulkley parameters are listed in Table 4.2. The results show that the longer chain PAC does have a larger impact on the shear stresses in the high shear rate range. PAC has a small impact on the yield stress compared to starches. Busch et al., (2018) found that aqueous PAC solutions do not exhibit yield stress. It is therefore possible that the increased amount of added particles is what increases the yield stress and not the PAC itself. In terms of Herschel-Bulkley parameters the surplus stress of Fluid 2 is significantly larger compared to those with added starch. Fluids with Ndril (5) and Dextrid (6) shows a very similar behavior with τ_s and n parameters being approximately equal. Fluid 4 displays a larger yield stress compared to Fluid 6.
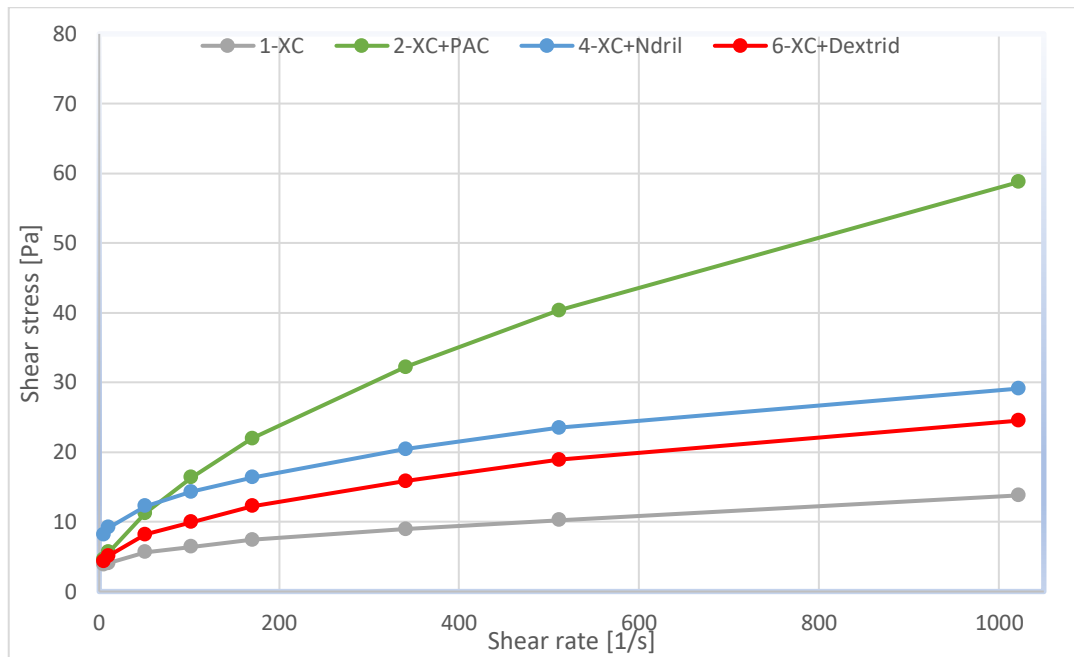
Figure 4.1.1: Flow curves for used polymer solutions.

Table 4.2: Obtained Herschel-Bulkley parameters for polymer solutions.

	1-XC	2-XC+PAC	4-XC+Ndril	6-XC+Dextrid
τ_y [Pa]	4.34	6.64	10.21	5.87
τ_s [Pa]	2.04	9.70	4.09	4.08
n	0.67	0.73	0.67	0.66

Figure 4.1.2 shows how different types of salt affects XC + PAC solutions. In this case it seems that $CaCl_2$ has a large effect on the solution, causing the structure to collapse. When testing Fluid 11 small particles of what seemed to be a mix of salt and PAC was observed. These kinds of observations were not observed when testing Ndril and different concentrations of $CaCl_2$. Fluid 2 are more resistant to NaCl and K_2SO_4, meaning that the bonds between XC and PAC weakens and destabilizes when exposed to divalent ions such as Ca^{2+}. 50 g of the given salt has been added for Fluid 3 and 11. Solutions containing potassium sulfate has a maximum SG of 1.083 (AMC drilling optimisation, 2019) equivalent to a weight percent of around 10%. Therefore, 35 g of K_2SO_4 has been used instead of 50 g. Fluid 3 seems to have a

higher viscosity than Fluid 2. Although one would expect slightly higher values with added salt, the increase is higher than expected. A significant amount of bubbles was present in Fluid 3, this may have contributed to higher shear stress measurements. Note that Fluid 2 and 12 overlaps in the figure.
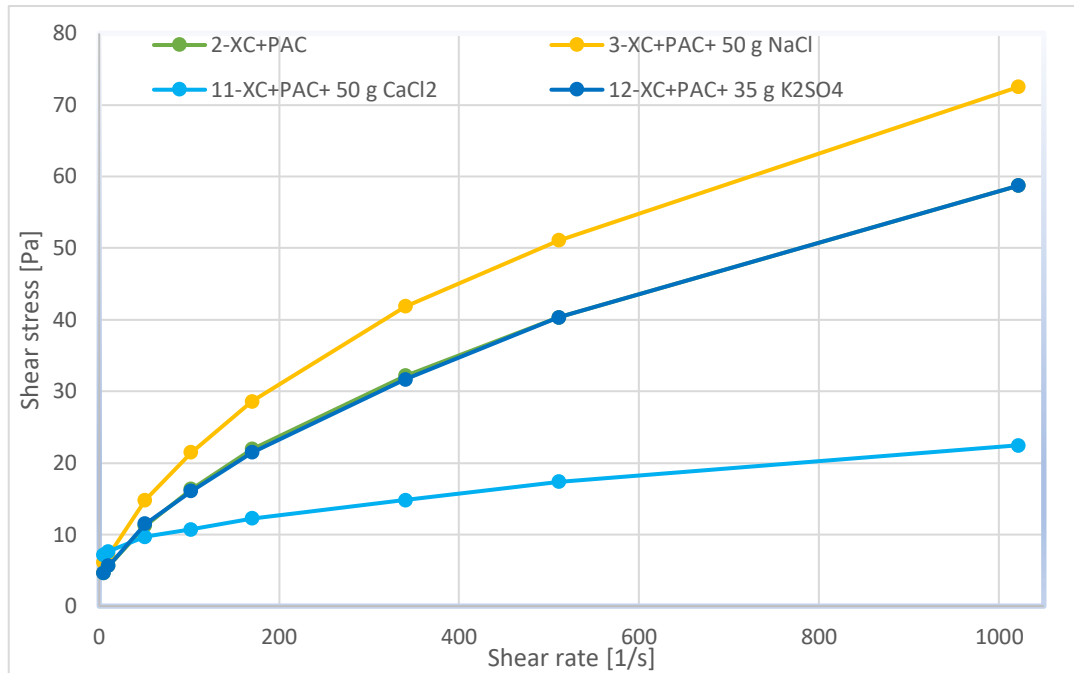
Figure 4.1.2: Flow curve of XC + PAC with different types of salt.

Like the samples using XC + PAC. Samples using XC + Ndril as a base, shows similar results for added NaCl and K_2SO_4 as shown in Figure 4.1.3. Differing from solutions containing PAC the structure does not collapse when exposed to $CaCl_2$. The added Ndril polymers reduces the calcium chlorides destructive behavior on XC. As Mateus & Rosângela (2019) found that using only XC, Ca^{2+} shrinks the structure of the molecule. Ndril therefore seems contribute to stabilizing XC. Common to all the samples with added salt is that the yield strength decreases.
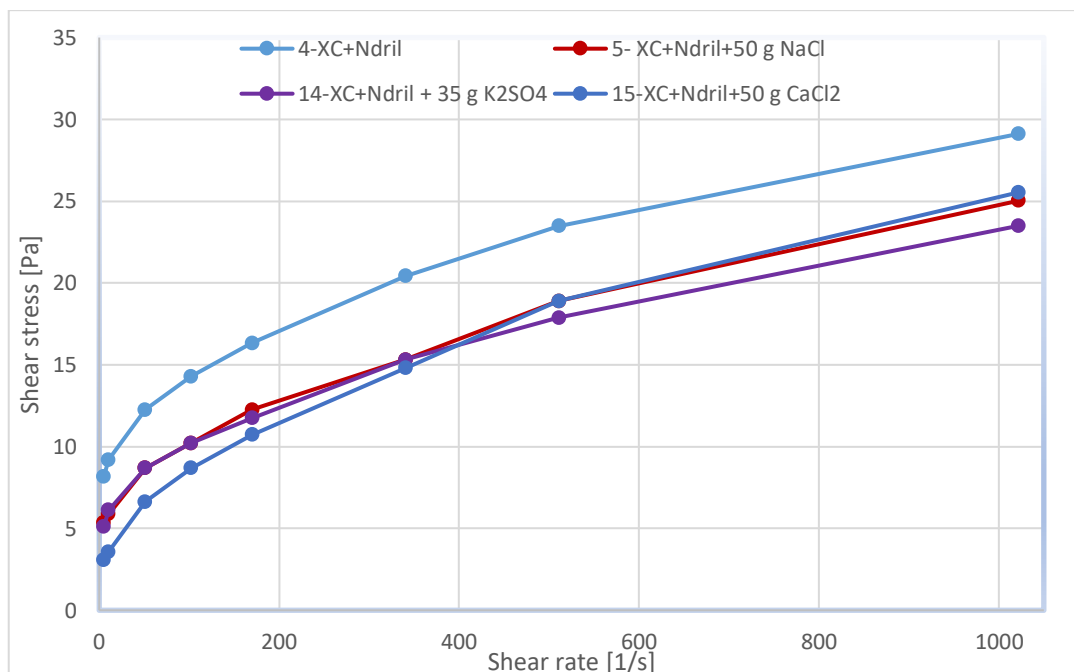
Figure 4.1.3: Flow curve of XC + Ndril with different types of salt.

Because Ndril proved to be more resistant to $CaCl_2$, other concentrations were tested to investigate its effect on the modified starch. The amount of 50 g was divided in half for one sample, giving 25 g. The other half were doubled giving 100 g. When adding 100 g $CaCl_2$ the fluid developed a consistency that reminds more of porridge. Showing signs that the electrostatic forces are starting to bind up the polymer. Also, the $CaCl_2$ solutions density increases, which is likely to have an impact on the results. The obtained flow curves are shown in Figure 4.1.4. The shear thinning index remains constant for all the fluids sitting at 10.67. The biggest change is the observed decrease in yield strength.
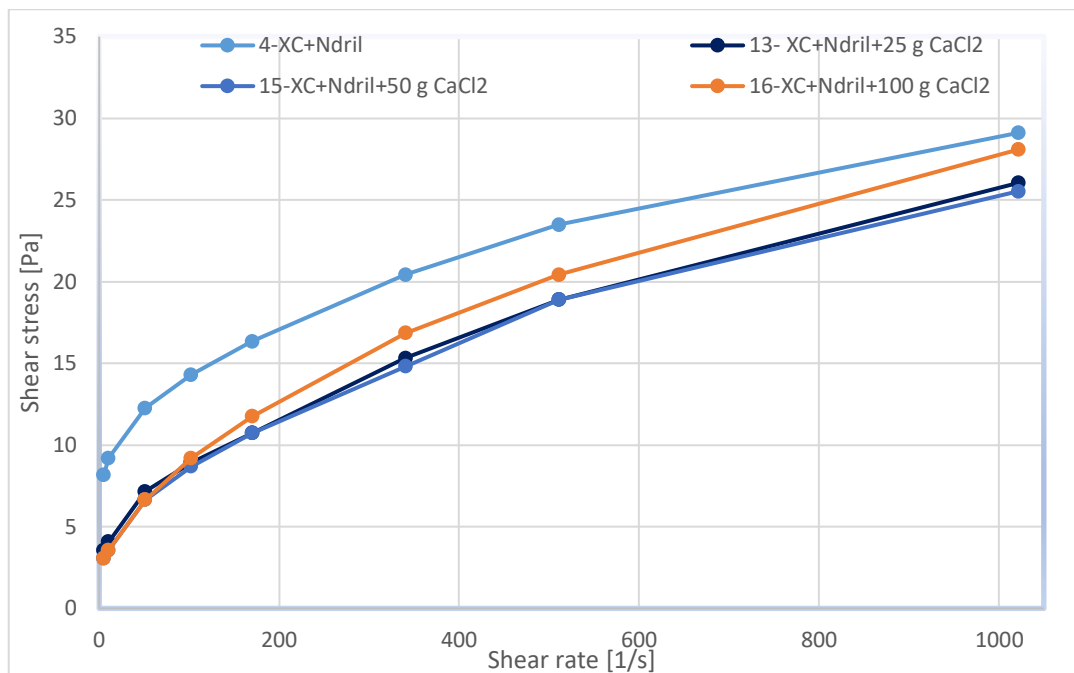
Figure 4.1.4: Flow curve of XC + Ndril with different concentrations of CaCl2.

The flow curves for the fluids with XC + Dextrid with added NaCl is shown in Figure 4.1.5. Similar to samples regarding Ndril, the yield strength decreases when exposed to NaCl. The other parameters remain approximately unchanged. Added Dextrid exhibits a smaller impact on the yield strength compared to XC and Ndril solutions. The results shows that NaCl decreases the yield stress properties of the solutions with XC + Ndril and XC + Dextrid weakens.
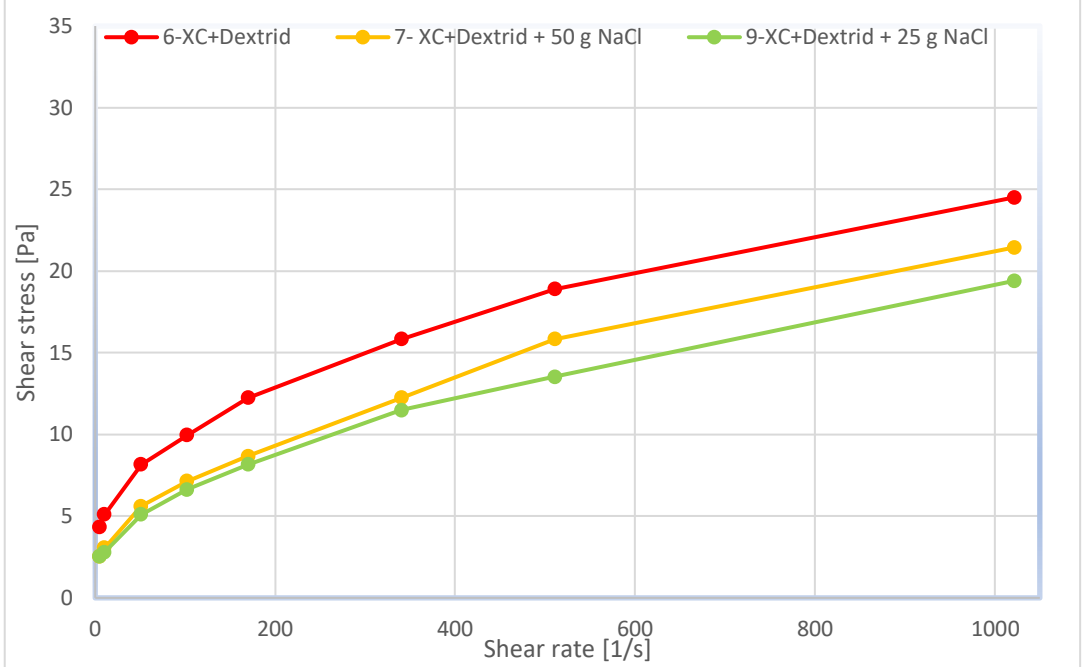
Figure 4.1.5: Flow curve of XC + Dextrid with different concentrations of NaCl.

In addition to the XC + Ndril with salt, a sample of Fluid 4 with added Auracoat UF was tested. With the results shown in Figure 4.1.6. Auracoat seems to have a small impact on the flow curve. The surplus stress increases slightly whilst the shear thinning factor decreases slightly. It is expected to see an elevated flow curve as Auracoat consists of bigger particles, which in turn will increase the shear stresses.
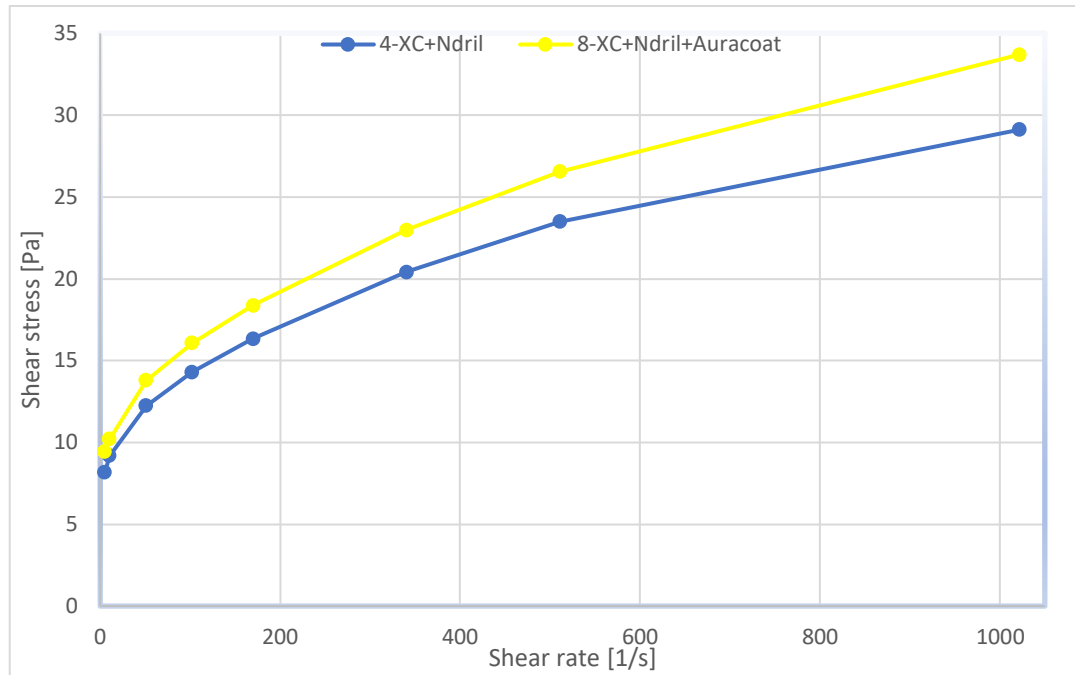
Figure 4.1.6: Flow curve of XC + Ndril & Auracoat UF.

A calculation of the Herschel-Bulkley parameters using the equations for all the tested fluids based on measurements from the concentric cylinder viscometer is listed in Table 4.3. The general impression is that the model suits the fluids well. Except for Fluid 11 were a structure destruction were observed. The model overestimates the high shear rate values.

Table 4.3: Modified Herschel Bulkley parameters for samples BHR.

Sample	τ_y [Pa]	τ_s [Pa]	n
1-XC	4.34	2.04	0.6651
2-XC + PAC	6.64	9.70	0.7298
3-XC + PAC + 50 g NaCl	8.17	13.28	0.6854
4-XC + Ndril	10.21	4.09	0.6651
5-XC + Ndril + 50 g NaCl	6.38	3.83	0.6872
6-XC + Dextrid	5.87	4.09	0.6592
7-XC + Dextrid + 50 g NaCl	3.57	3.57	0.6990
8-XC + Ndril + Auracoat	10.98	5.11	0.6484
9-XC + Dextrid + 25 g NaCl	3.06	3.57	0.6601
10-XC + Ndril + 25 g NaCl	7.15	3.83	0.7104
11-XC + PAC+ 50 g CaCl$_2$	6.13	5.36	0.5809
12-XC + PAC+ 35 g K$_2$SO$_4$	6.64	9.45	0.7414
13-XC + Ndril + 25 g CaCl$_2$	4.60	4.34	0.6938
14-XC+Ndril + 35 g K$_2$SO$_4$	7.15	3.06	0.7270
15-XC+Ndril+50 g CaCl$_2$	4.09	4.60	0.6690
16-XC+Ndril+100 g CaCl$_2$	4.09	5.11	0.6721

4.2 Mechanical and Thermal Wear

The fluids containing PAC shows the largest variation in viscosity data. Adding 50 g NaCl seems to rise the flow curve as shown in Figure 4.2.1. It also increases the stability compared to Fluid 2. Note that some bubbles were observed in Fluids 2 and 3 which may influence the measurements done before hot rolling. One would especially expect a lower curve for Fluid 3.
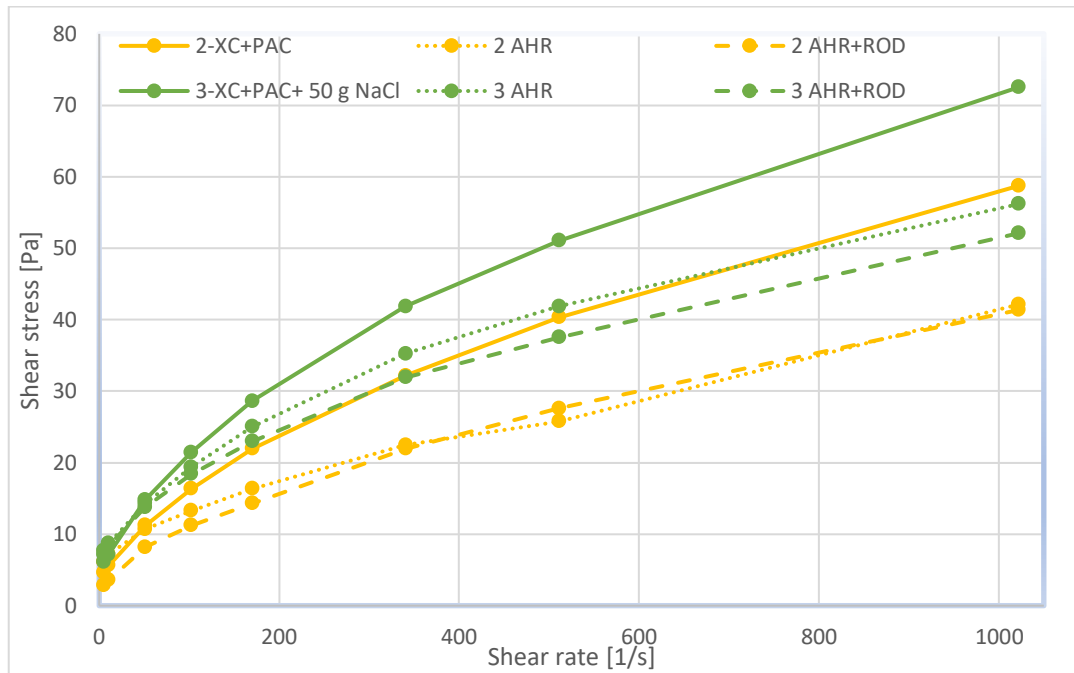
Figure 4.2.1: Flow curve of XC + PAC + NaCl AHR

Tests using K_2SO_4 shows a similar behavior to the tests using NaCl. It seems to be less prone to degradation when exposed to higher temperatures and mechanical wear. Of the different types of salt used in combinations with PAC, K_2SO_4 shows a better resistance against mechanical wear compared to NaCl. Figure 4.2.2 shows the obtained results AHR with and without rod XC and PAC combinations with different types of salt.
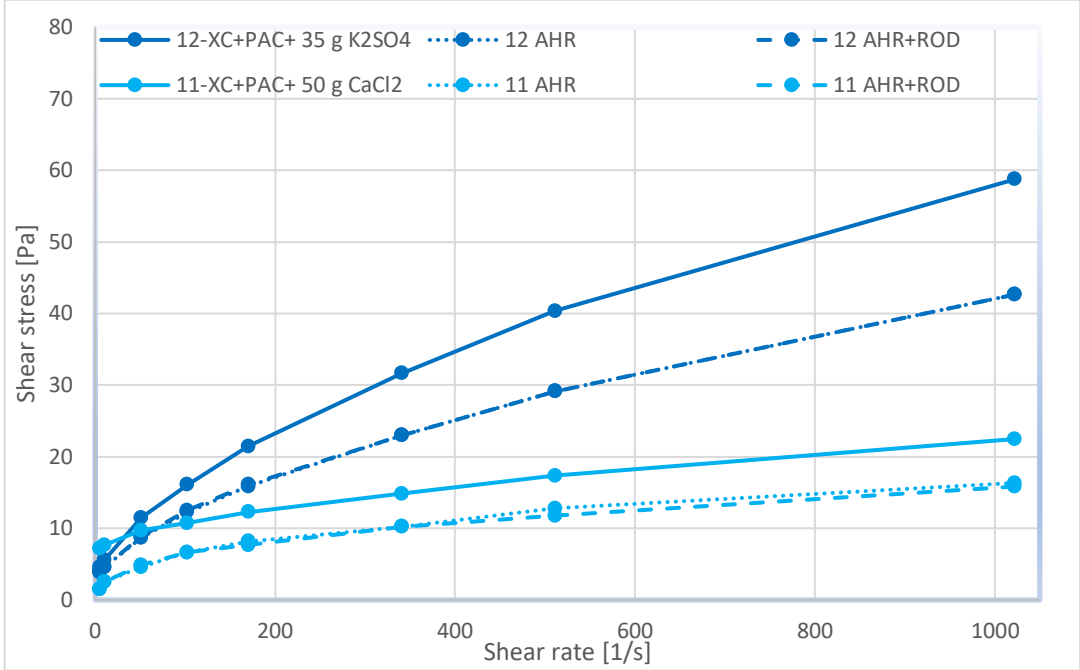
Figure 4.2.2: Flow curve of XC + PAC + K_2SO_4 and XC + PAC + $CaCl_2$ AHR

As expected from the measurements BHR, the flow curve of Fluid 11 drops further AHR. It seems that the PAC coils up as we are now at a level close to the base fluid containing only XC.

Figure 4.2.3 shows the effect of NaCl on the Ndril starch. The effect of salt is now a lower decrease in the flow curve. The sodium chloride makes the XC and Ndril more robust against high temperature and mechanical wear.
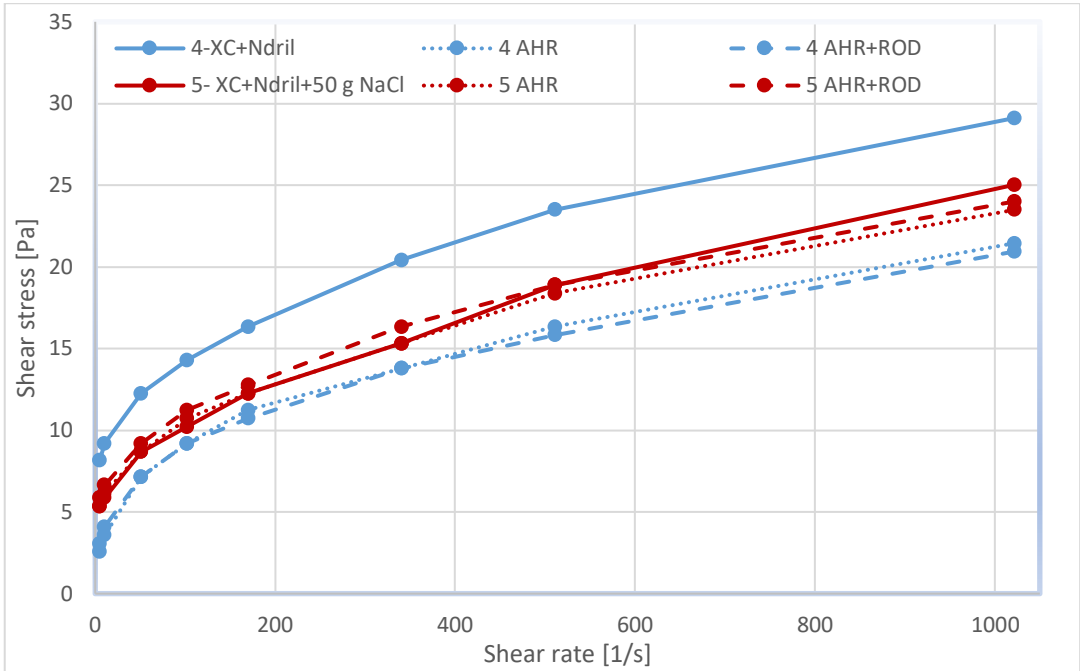
Figure 4.2.3: Flow curve of XC + Ndril + 50 g NaCl AHR.

Solutions containing XC and Ndril also proved to be resistant against $CaCl_2$ as shown in Figure 4.2.4. The concentration of calcium chloride has a negligible effect on the obtained numbers. Values at high shear rates are more reduced AHR compared to values at low shear rates. Meaning that their curvature index decreases, and it has a lower viscosity at higher shear rates.
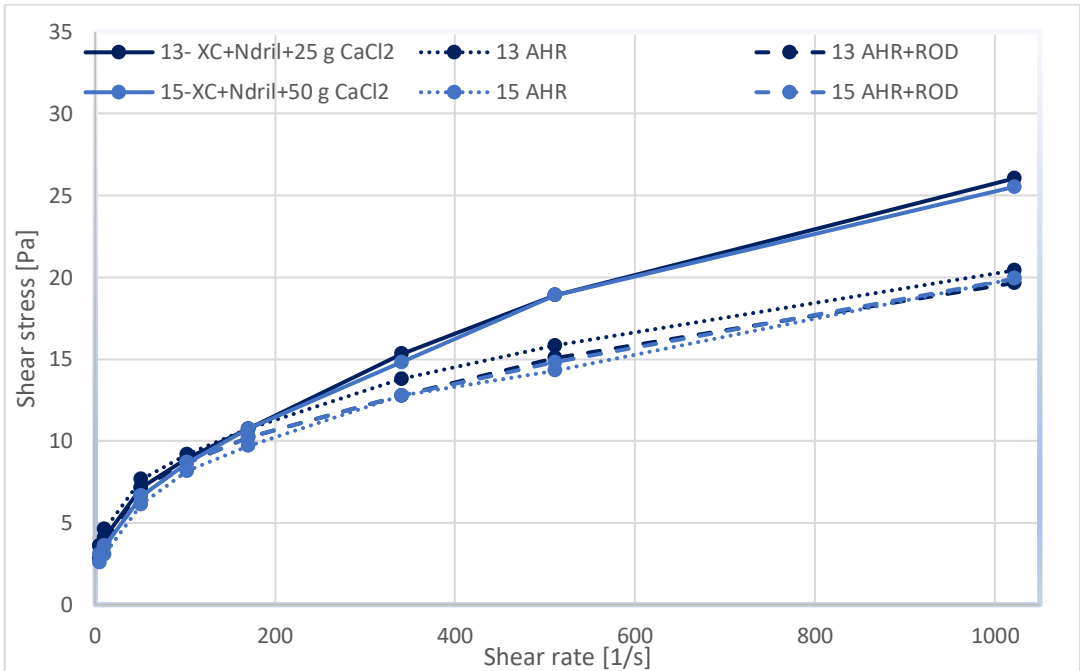
Figure 4.2.4: Flow curve of XC + Ndril with different concentrations of $CaCl_2$ AHR.

From Figure 4.2.5 we see that the yield strength drops AHR both with and without rod for Fluid 8. The fluid shows a good resistance against mechanical wear. The temperature is what seems to have the most effect on the fluid. The τ_s and the n parameters remains relatively unchanged. Auracoat seems to have a small effect on the resistance against thermal and mechanical wear. Auracoat consist of larger particles compared to the other polymers, making it more likely that sag particles have been present in the bottom of the fluid. This is expected to affect the results for Fluid 8 AHR to a larger degree than other samples involving smaller particles. These differences are expected to be smaller if the fluid is re-mixed AHR.
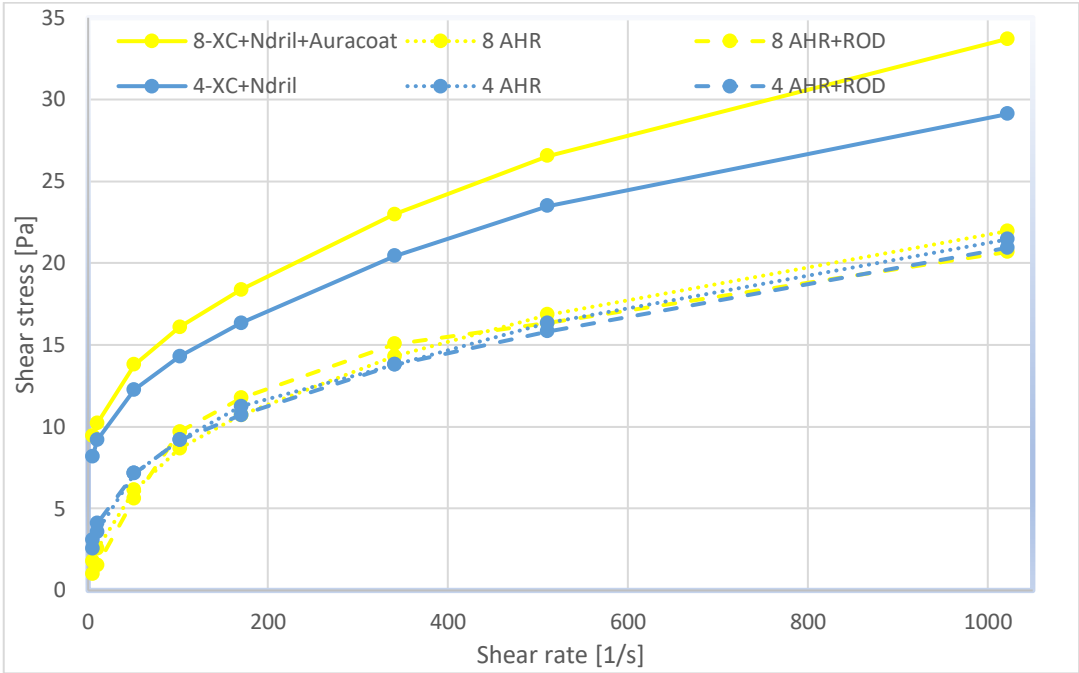
Figure 4.2.5: Flow curve of XC + Ndril + Auracoat AHR.

For solutions involving XC and Dextrid, added NaCl seems to have a similar effect to the obtained results for solutions with XC and Ndril. Figure 4.2.6 shows that Fluid 7 becomes more robust against the mechanical and thermal wear. The yield strength does not drop as significantly as for Fluid 6. The amount of salt does not seem to be defining for the results. As a sample with 25 g added NaCl had the same results as for Fluid 7. This can be observed upon checking the values in Table 4.4.
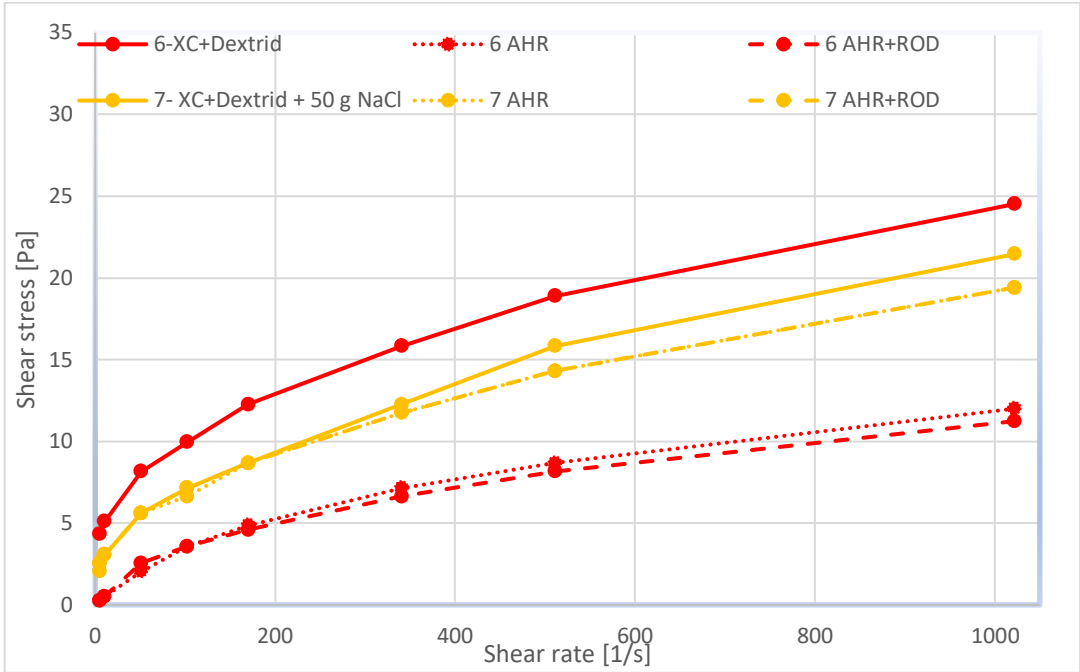
Figure 4.2.6: Flow curve of XC + Dextrid + 50 g NaCl AHR

From the discussed results we see that in general fluids without added salt or other additives degrades more than those with added salt. The largest decrease in shear stresses is observed at the lower range of shear stresses. When analyzing the modified Herschel-Bulkley parameters, the biggest observed changes are for the yield stress values. Solutions involving XC and starch polymer had a decrease in yield stress AHR. The samples are constructed with small particles. This could be a reason why small changes for tests with and without rod were observed. For sample 2 the effect of the rod is larger as PAC is a longer chain polymer than starch polymers.

Table 4.4: Modified Herschel-Bulkley parameters for samples AHR.

Sample	τ_y [Pa]	τ_s [Pa]	n
1-XC	4.34	2.04	0.6651
1-AHR	1.02	2.30	0.5740
1-AHR+ROD	1.53	1.79	0.5119
2-XC + PAC	6.64	9.70	0.7298
2-AHR	8.17	5.11	0.5441
2-AHR+ROD	4.34	6.89	0.5816
3-XC + PAC + 50 g NaCl	8.17	13.28	0.6854
3-AHR	9.70	9.70	0.5441
3-AHR+ROD	9.70	8.68	0.5041
4-XC + Ndril	10.21	4.09	0.6651
4-AHR	4.60	4.60	0.6154
4-AHR+ROD	5.11	4.09	0.5883
5-XC + Ndril + 50 g NaCl	6.38	3.83	0.6872
5-AHR	6.89	3.83	0.6368
5-AHR+ROD	7.41	3.83	0.6368
6-XC+Dextrid	5.87	4.09	0.6592
6-AHR	0.77	2.81	0.4393
6-AHR+ROD	0.77	2.81	0.4087
7-XC + Dextrid + 50 g NaCl	3.57	3.57	0.6990
7-AHR	4,09	2.55	0.6320
7-AHR+ROD	3.57	3.57	0.6463
8-XC + Ndril + Auracoat	10.98	5.11	0.6484
8-AHR	3.32	5.36	0.5623
8-AHR+ROD	2.04	7.66	0.5623
9-XC + Dextrid + 25 g NaCl	3.06	3.57	0.6601
9-AHR	4.34	2.55	0.5781
9-AHR+ROD	3.57	3.32	0.6173
10-XC + Ndril + 25 g NaCl	7.15	3.83	0.7104
10-AHR	6.13	4.09	0.6232
10-AHR+ROD	7.66	3.06	0.6021
11-XC + PAC + 50 g CaCl2	6.13	5.36	0.5809
11-AHR	3.57	3.06	0.3768
11-AHR+ROD	3.57	3.06	0.3590
12-XC + PAC + 35 g K2SO4	6.64	9.45	0.7414
12-AHR	5.36	6.89	0.5962
12-AHR+ROD	5.11	7.41	0.5991
13-XC + Ndril + 25 g CaCl2	4.60	4.34	0.6938
13-AHR	5.62	3.57	0.5330
13-AHR+ROD	4.85	3.83	0.5330

14-XC + Ndril + 35 g K2SO4	7.15	3.06	0.7270
14-AHR	6.13	3.57	0.6842
14-AHR+ROD	6.64	3.06	0.6690
15-XC + Ndril + 50 g CaCl2	4.09	4.60	0.6690
15-AHR	3.57	4.60	0.5509
15-AHR+ROD	4.09	4.60	0.5371
16-XC + Ndril + 100 g CaCl2	4.09	5.11	0.6721
16-AHR	3.57	5.62	0.6435
16-AHR+ROD	2.30	4.34	0.6180

4.3 Amplitude Sweeps Using Rheometer

Amplitude sweeps has been performed on fluids 1, 2, 3, 4, 5, 8, 11 and 15 using the Anton Paar 302 MCR rheometer. Figure 4.3.1 shows the obtained results for Fluid 1. The value denoted as tau in the diagram is the flow point τ_f that is the point where G' = G''. The value denoted as G' in the plot is the storage modulus of the fluid at the flow point. τ_y is calculated using regression models in the RheoCompass software and is shown as "tau" in the plots. The yield stress is the point where this drops by 3% of the original G'. One should note that at low shear stresses, there is some noise causing the G' values to change. These points are left out of the calculation of the yield stress but are visible in the diagram to show the noise. A good experimental curve is obtained if G' and G'' remains constant before start.
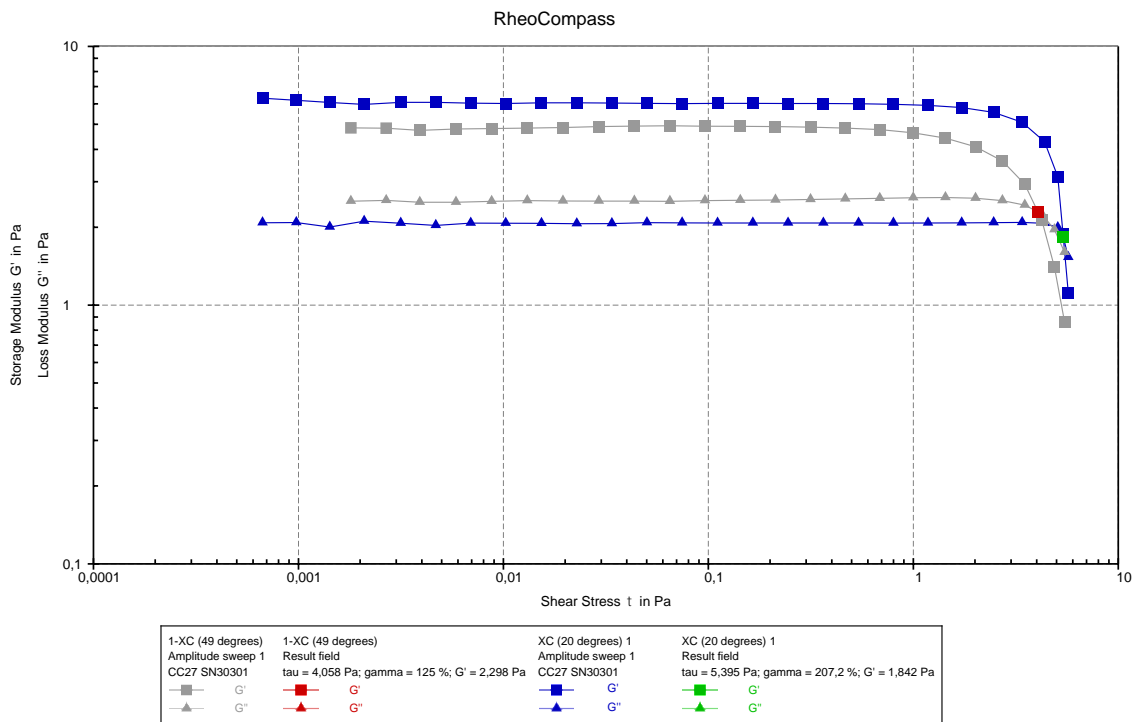
Figure 4.3.1: Amplitude sweep: 1-XC.
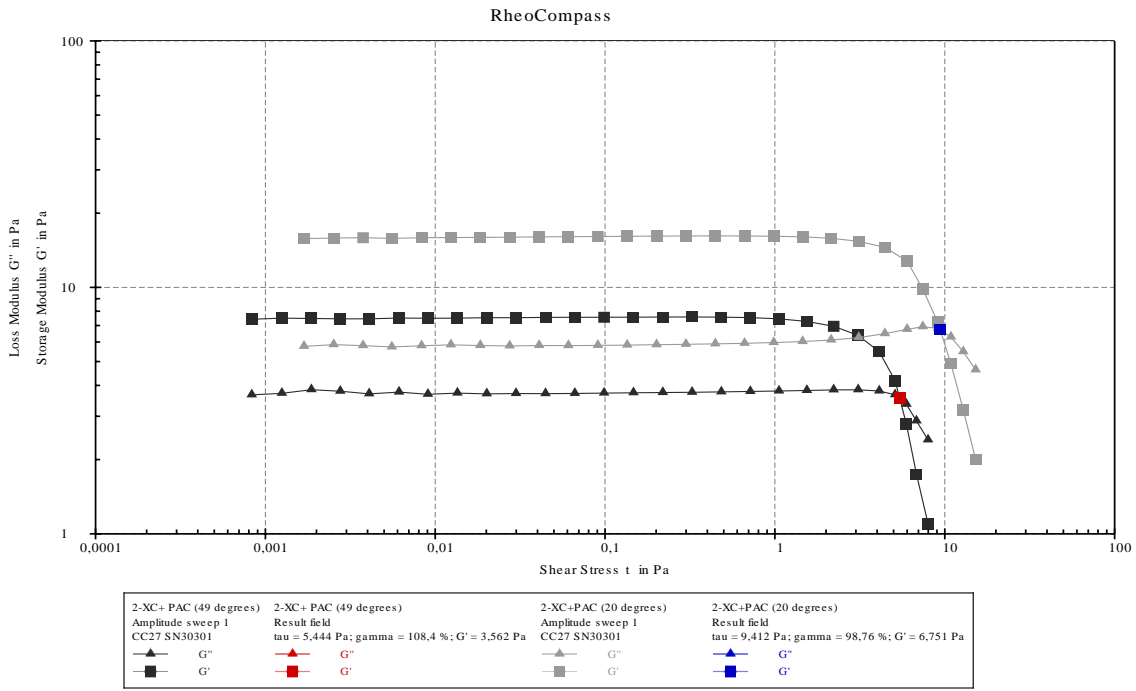
Figure 4.3.2: Amplitude sweep: 2-XC + PAC.

From Figure 4.3.3 and Figure 4.3.4 we get a better view of how the different types of salt affect the XC + PAC solution shown in Figure 4.3.2. The added NaCl has a negligible effect on the flow point. The NaCl has a larger impact at higher shear rates. The added $CaCl_2$ decreases the flow point. G' increases slightly compared to fluids 2 and 3 meaning it can store a higher amount of energy during deformation.
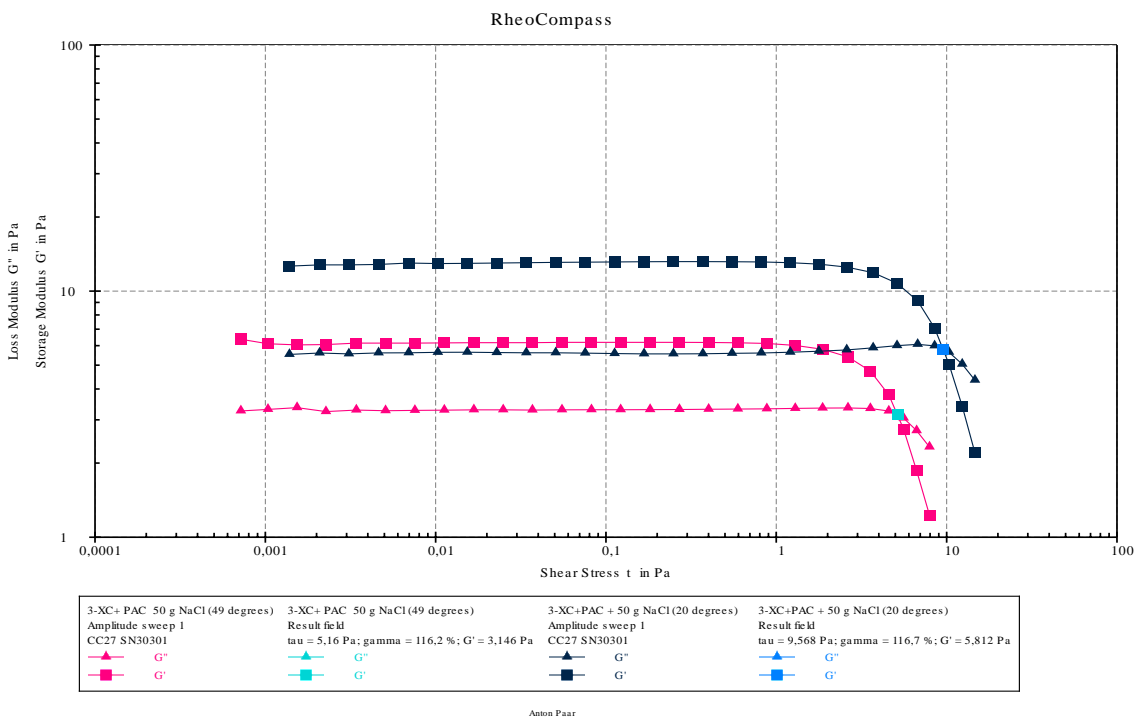
Figure 4.3.3: Amplitude sweep: 3-XC + PAC + 50 g NaCl.
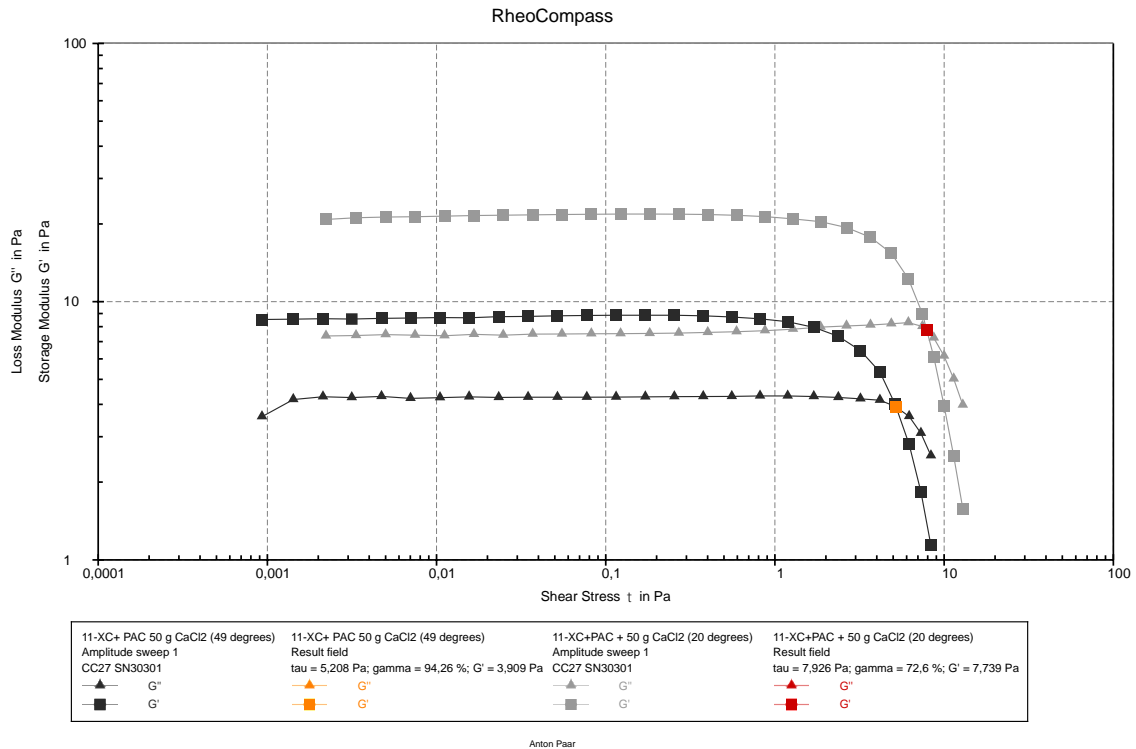
Figure 4.3.4: Amplitude sweep: 11-XC + PAC + 50 g CaCl₂.

Fluid 4 has a smaller decrease in the flow point compared to Fluid 2 and shows a lower decrease in G' after testing at 49 °C as shown in Figure 4.3.5. PAC is compatible to higher temperatures than Ndril. The results shows that XC + Ndril solutions is more stable when dealing with temperatures under its decomposition temperature.
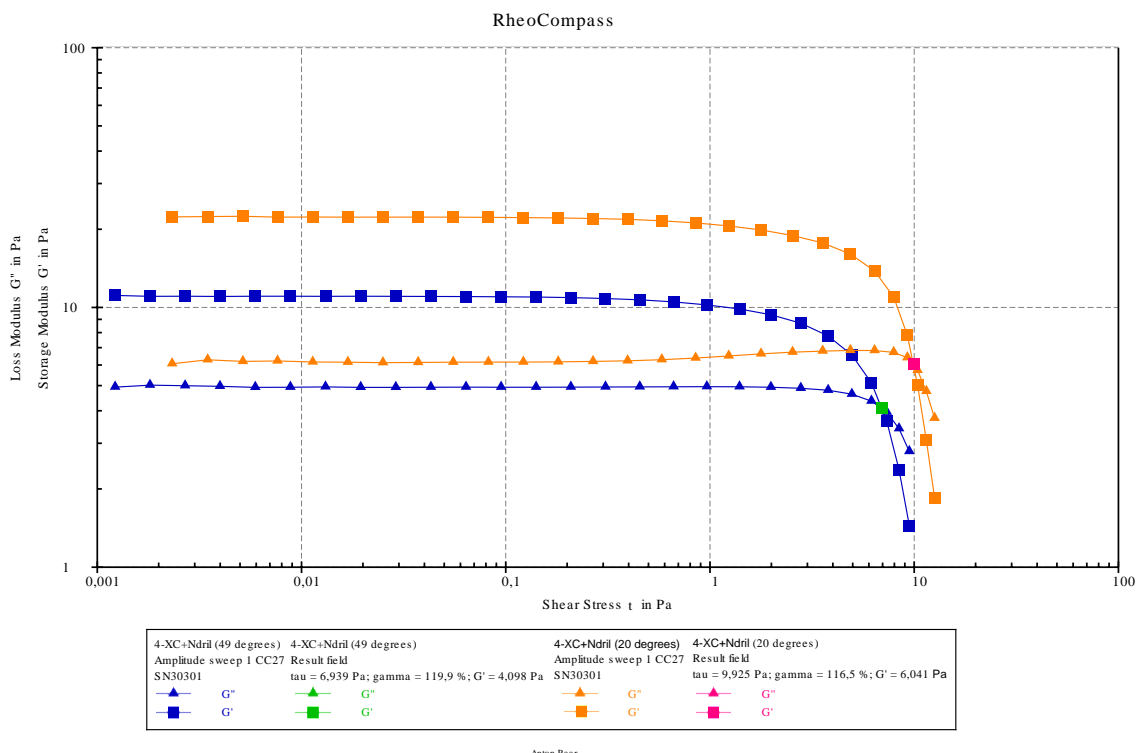
Figure 4.3.5: Amplitude sweep: 4-XC + Ndril.

5-XC+Ndril + 50 g NaCl (49 degrees)	5-XC+Ndril + 50 g NaCl (49 degrees)	5-XC+Ndril + 50 g NaCl (20 degrees)	5-XC+Ndril + 50 g NaCl (20 degrees)
Amplitude sweep 1	Result field	Amplitude sweep 1	Result field
CC27 SN30301	tau = 7,09 Pa; gamma = 101,1 %; G' = 4,967 Pa	CC27 SN30301	tau = 9,132 Pa; gamma = 85,58 %; G' = 7,561 Pa
▲ G"	▲ G"	▲ G"	▲ G"
■ G'	■ G'	▲ G'	■ G'

Anton Paar
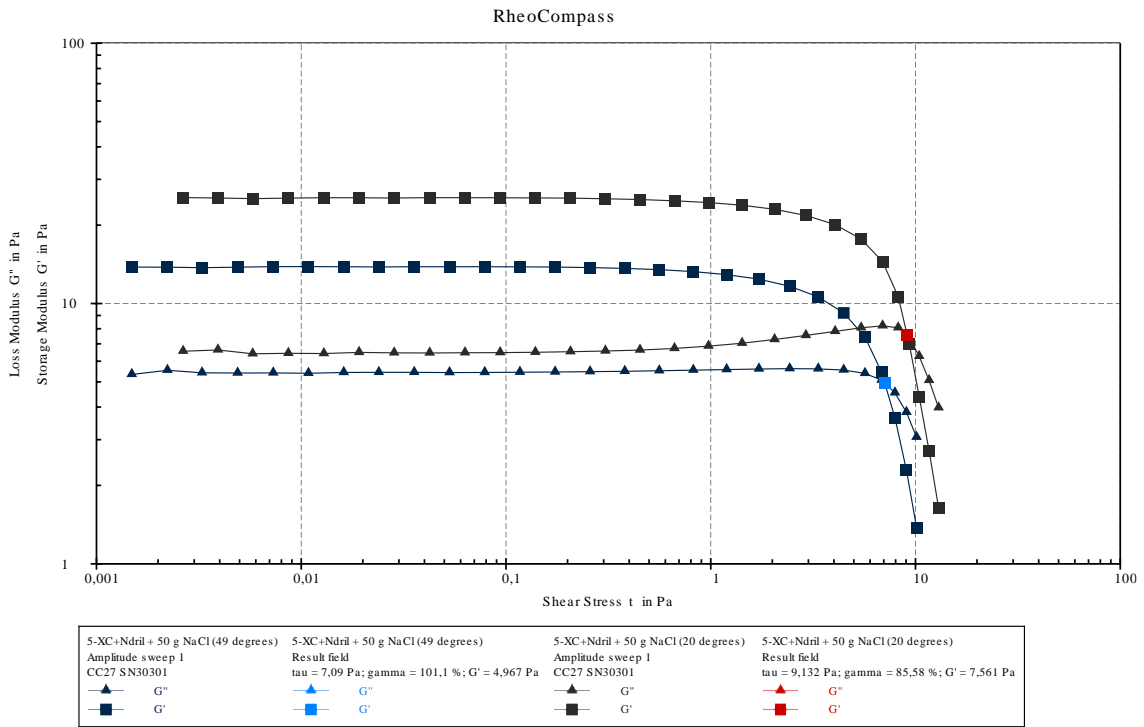
Figure 4.3.6: Amplitude sweep: 5-XC + Ndril 50 g NaCl.

Figure 4.3.7 shows the obtained AS results for Fluid 15. The added $CaCl_2$ increases the flow point compared to fluids 5 (Figure 4.3.6) and 4. This indicates that the divalent Ca^{2+} ions form stronger bonds with the polymers. It was observed that the structure of Fluid 15 became more gel like compared to the other fluids.

15-XC+Ndril + 50 g CaCl2 (49 degrees)	15-XC+Ndril + 50 g CaCl2 (49 degrees)	15-XC+Ndril + 50 g CaCl2 (20 degrees) 1	15-XC+Ndril + 50 g CaCl2 (20 degrees) 1
Amplitude sweep 1	Result field	Amplitude sweep 1	Result field
CC27 SN30301	tau = 7,878 Pa; gamma = 109,7 %; G' = 5,081 Pa	CC27 SN30301	tau = 11,31 Pa; gamma = 101,8 %; G' = 7,867 Pa
▲ G"	▲ G"	▲ G"	▲ G"
■ G'	■ G'	■ G'	■ G'

Anton Paar
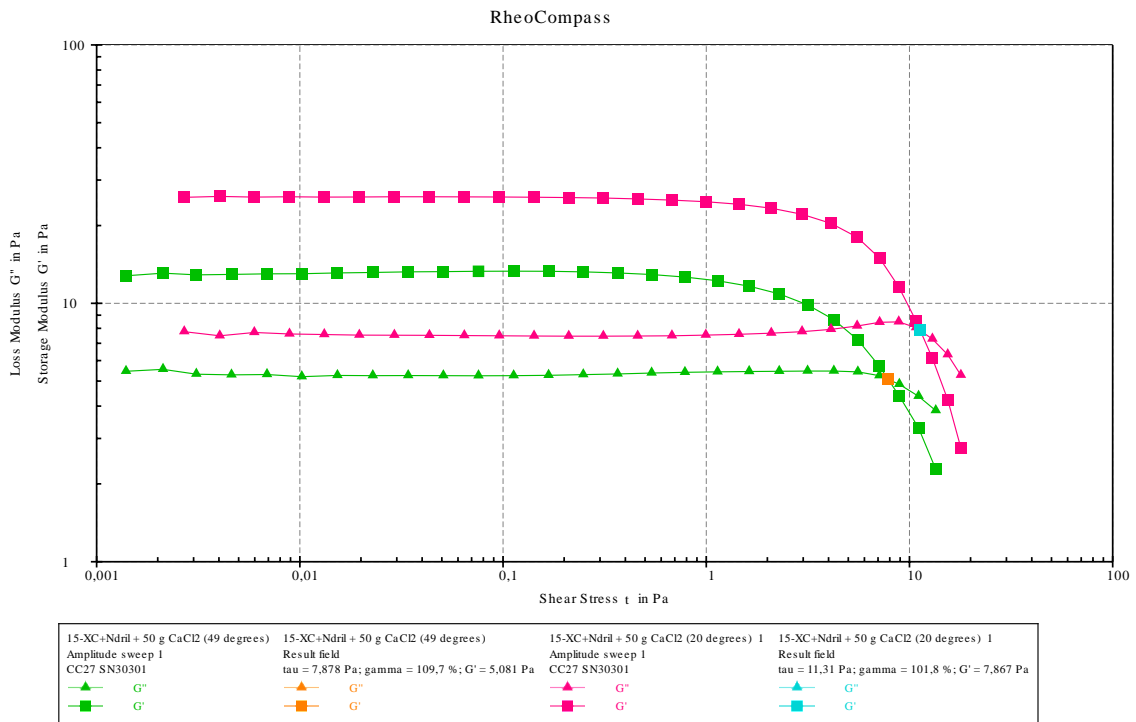
Figure 4.3.7: Amplitude sweep: 15-XC + Ndril 50 g CaCl2.

Figure 4.3.8 shows the results for Fluid 8. Compared to XC + Ndril the Auracoat increases the flow point, however the yield point is decreased for temperatures of 20 °C. This relation shifts for temperatures of 49 °C and the yield point is higher for Fluid 8. The results tell us that the Auracoat seems to increase the thermostability of the XC & Ndril solution.
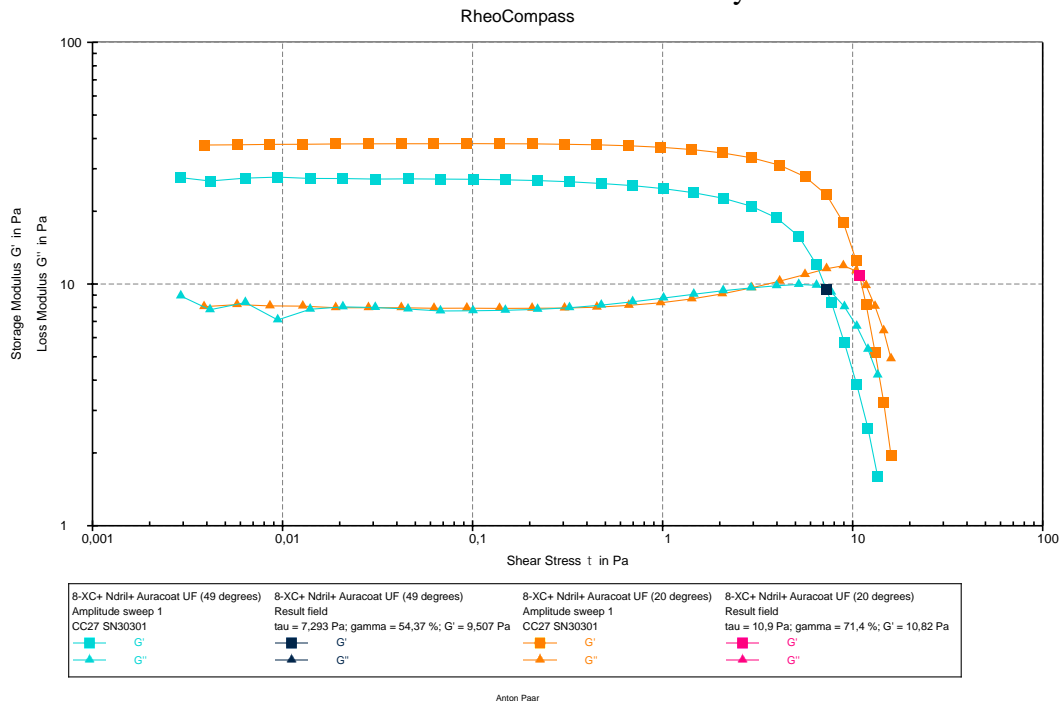
Figure 4.3.8: Amplitude sweep: 8-XC + Ndril + Auracoat UF

All obtained values for amplitude sweep tests performed on the rheometer is listed in Table 4.5. As was the case for tests done with the Ofite viscometer, when Fluid 2 is exposed to $CaCl_2$ the flow point and yield point decreases. The general observation is that the storage modulus decreases at higher temperatures. The same applies for the flow point and the yield point, however the storage modulus increases slightly for Fluid 1. XC + Ndril solutions shows a larger effect in the LVE region of the fluids compared to XC + PAC solutions. Verifying that PAC has a better thermostability than Ndril. Fluid 8 puts itself in the middle of Fluid 4 with just Ndril, and above those with Ndril and added salts. Like the results obtained with the simpler viscometer.

Table 4.5: Results from Amplitude sweep tests.

	20 °C			49 °C		
Sample	τ_f [Pa]	τ_y [Pa]	G' [Pa]	τ_f [Pa]	τ_y [Pa]	G' [Pa]
1-XC	5.395	1.02	1.842	4.058	0.656	2.298
2-XC + PAC	9.412	2.75	6.751	5.444	1.44	3.561
3-XC + PAC + 50 g NaCl	9.568	1.80	5.812	5.160	1.33	3.146
11-XC + PAC + 50 g $CaCl_2$	7.926	0.977	7.739	5.208	0.722	3.909
4-XC + Ndril	9.925	2.98	6.041	6.939	0.544	4.098
5-XC + Ndril + 50 g NaCl	9.132	0.99	7.561	7.090	0.700	4.967
15-XC + Ndril + 50 g $CaCl_2$	11.31	0.970	7.867	7.878	0.533	5.081
8-XC + Ndril + Auracoat UF	10.90	1.22	10.82	7.293	0.830	9.507

The results shows that the solutions gel strength reduces at 20 °C when exposed to different types of salts like Mateus & Rosângela (2019) found. It is observed that the gel strength of XC + PAC increases compared to Fluid 1. As mentioned in the theorethical

background chapter aqueous PAC solutions exhibit none to minimal yield strength. XC and PAC do therefore seem to bond due to the increased yield strenght. But the bonds are weaker than XC and starch bonds which increases all three parameters. When analyzing the obtained data at temperatures of 49° C. We observe the effect $CaCl_2$ has on the XC + PAC solution with a noticeably lower yield strength. The flow point remains close to fluid 2 and 3. G' at the flow point is also higher for Fluid 11 compared to Fluid 2 and 3. PAC is expected to have low contributions on the yield strength. Therefore, the bonds between salts, xanthan gum and water molecules are probably the main contributors to the observed changes.

For solutions of XC + Ndril the different additives increase the discussed parameters, and the viscosifying effect seems to decrease at higher temperatures. Auracoat reduces the reduction in yield strength of the fluid at temperatures of 49° C. For higher temperatures, the effect of Ndril in the LVE region decreases. The results shows that the mix of XC and salt becomes more dominant. Being the main contributor for the results. The same is observed for Auracoat.

The tests using the rheometer does of course show other results than what is obtained with the concentric cylinder viscometer. As the yield stress is the end of the LVE region for the measurements at the rheometer. It is defined different from the definition used in the modified Herschel-Bulkley model. Therefore, the yield stress of the fluids is lower in the amplitude sweeps. However, when examining the flow points with the calculated yield stress. The values are more similar and matches better for the flow point when comparing with the calculated yield stress from the viscometer. This is illustrated in Table 4.6, where the relation between obtained yield stress from viscometer measurements and τ_f or τ_y, 100% illustrates a perfect fit.

Table 4.6: Calculated yield stress using viscometer readings divided by measured value with rheometer using amplitude sweep.

Sample	τ_y [Pa]	τ_f [Pa]
1-XC	425.6 %	80.5 %
2-XC + PAC	241.4 %	70.5 %
3-XC + PAC + 50 g NaCl	291.8 %	85.4 %
11-XC + PAC + 50 g $CaCl_2$	342.8 %	102.9 %
4-XC + Ndril	644.8 %	69.9 %
5-XC + Ndril + 50 g NaCl	900.0 %	100.7 %
15-XC + Ndril + 50 g $CaCl_2$	627.3 %	61.7 %
8-XC + Ndril + Auracoat UF	421.2 %	36.1 %

4.4 Flow Curves Using Rheometer

The results obtained with the rheometer is proving to be more accurate than what is obtained from the concentric cylinder viscometer. The concentric cylinder viscometer is more unstable at lower shear rates (Sele, 2023). The fewer and more inaccurate measurement points at lower shear rates makes the obtained plots with the Ofite Viscometer more exposed to noise and inaccuracy. The data from the rheometer looks better compared to the viscometer, with the points laying in a visually satisfying line.
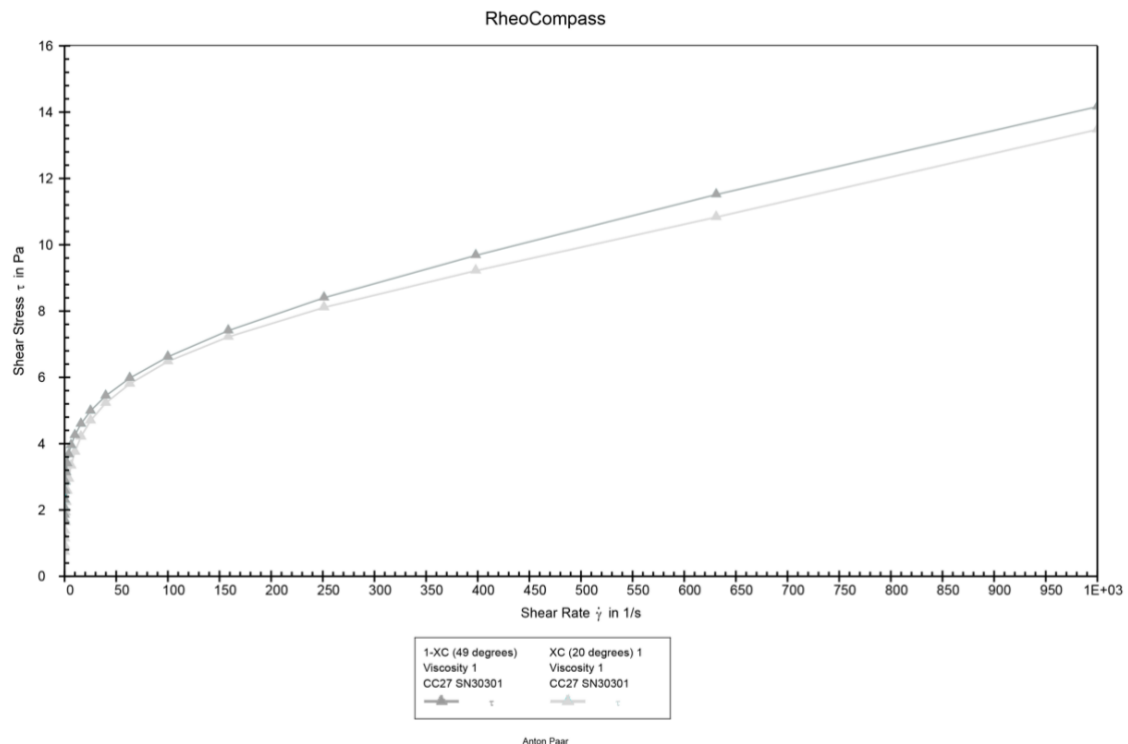
Figure 4.4.1: Flow curve of XC + PAC (rheometer data).

Comparing Figure 4.4.1 with the results with the equivalent values from Figure 4.1.1. The obtained values look very similar in the range of 100 to 1000 1/s. But with larger differences in the low shear rate under 100 1/s. Figure 4.4.2 shows the obtained flow curve for Fluid 11. This is the biggest difference compared to what was obtained using the concentric cylinder viscometer. With noticeably higher shear stresses. Due to such different results, it seems that Fluid 11 is unstable and difficult to measure. Because of this, the rheometer should be conclusive for tests of Fluid 11 BHR. Fluids 2 and 3 both start to "break" of at around 10 Pa. The largest observed differences in shear stress are present at shear rates higher than 100 1/s. Fluid 3 using added NaCl does not have a significant impact on the flow curve. Other than the increased resistance against mechanical and thermal wear documented earlier.
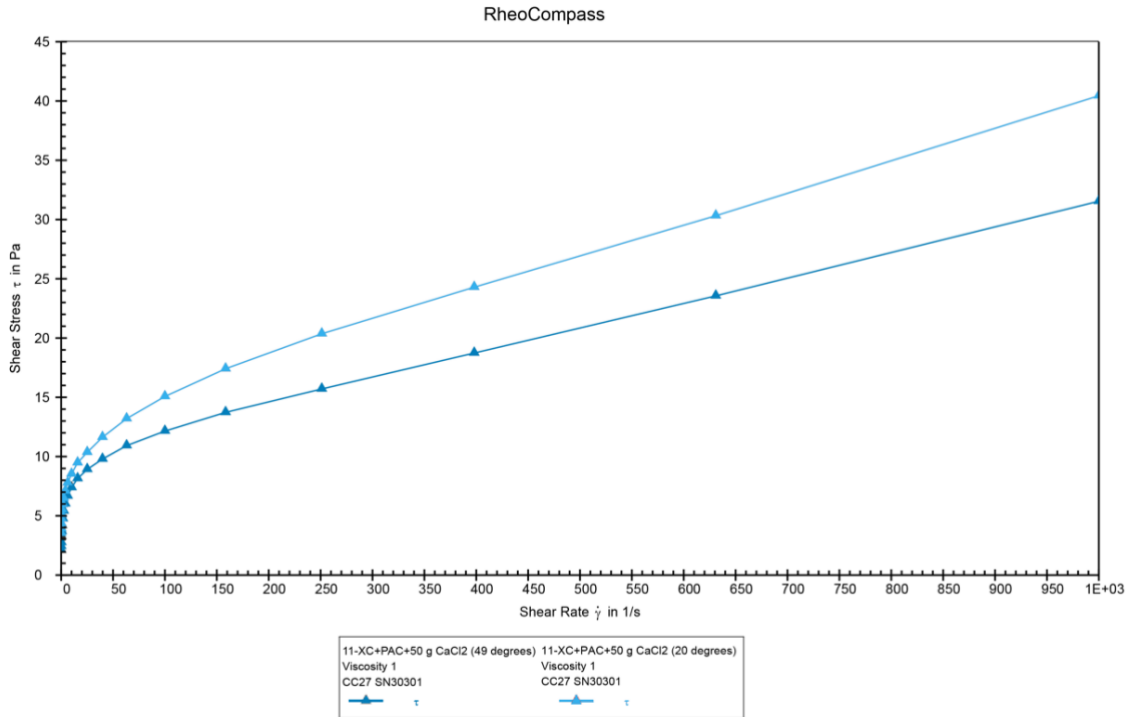
Figure 4.4.2: Flow curve of XC + PAC + 50 g CaCl$_2$ (rheometer data).

As for Fluid 4, flow curves at 49 °C confirms the decreased thermostability as measured with the amplitude sweeps with the fluid starting. XC + Ndril also shows a significant decrease in shear stress at low shear rates. Comparing to the data obtained with the concentric viscometer. The concentric viscometer does not show the transition zone where the fluid starts to break of and becoming more linear. For Fluid 8 the thermostability is significantly increased as showed in Figure 4.4.4. The low shear rate points are now overlapping at both temperatures. Auracoat does therefore camouflages the reduced thermostability of Ndril. In general, Auracoat has small effects on the viscosity at 20 °C despite a significant increase in the number of particles. The flow curves for fluids 1, 3, 5 and 11 are attached in Appendix F.
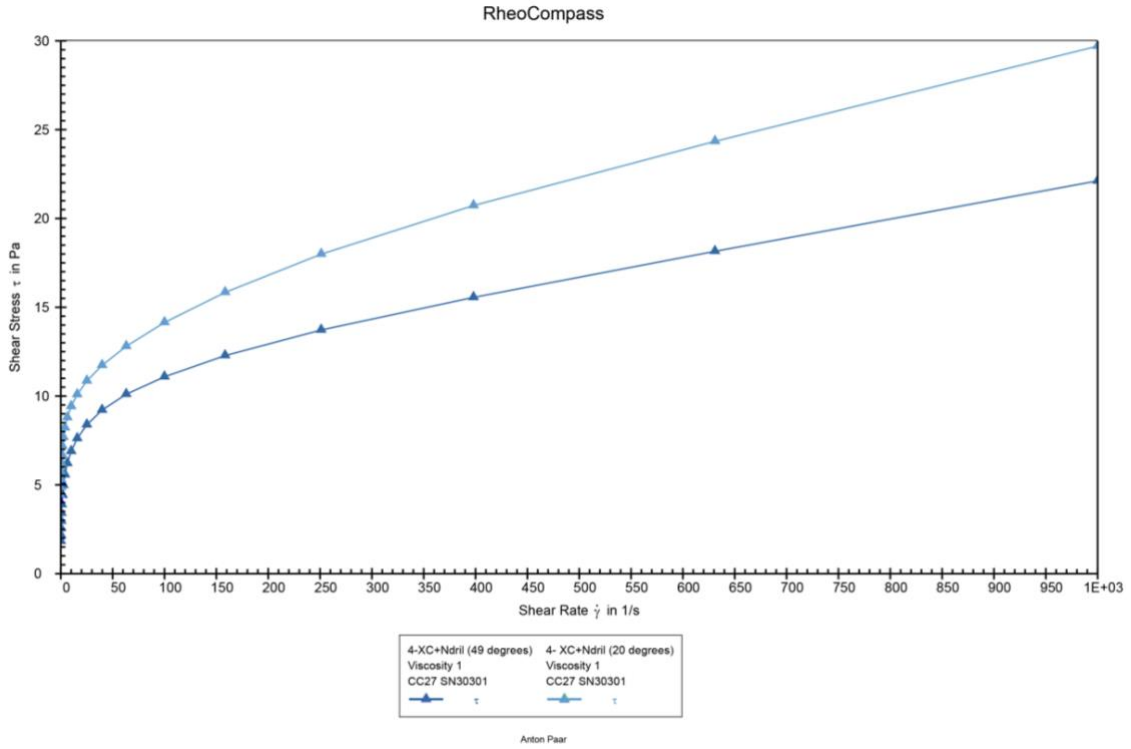
Figure 4.4.3: Flow curve of XC + Ndril (rheometer data).
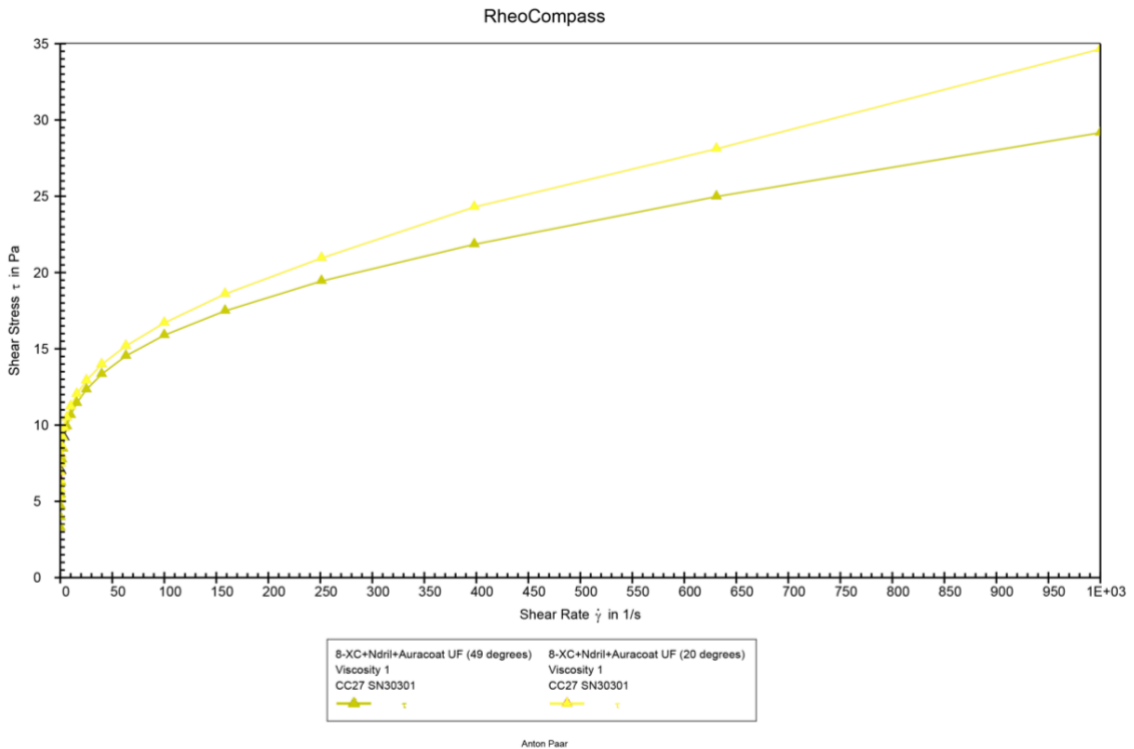
Figure 4.4.4: Flow curve of XC + Ndril + Auracoat UF (rheometer data).

Added $CaCl_2$ to XC + Ndril does not show the decreased values as for fluid 4 and 5 as shown in Figure 4.4.5. τ at 49 °C increases compared to at 20 °C in the low shear rate range. Putting this in context with the previously obtained results this is mainly due the interactions between XC, water and $CaCl_2$. The effect is not as significant for XC + PAC as Pac is an anionic polymer. Thus, also binding Ca^{2+} ions.
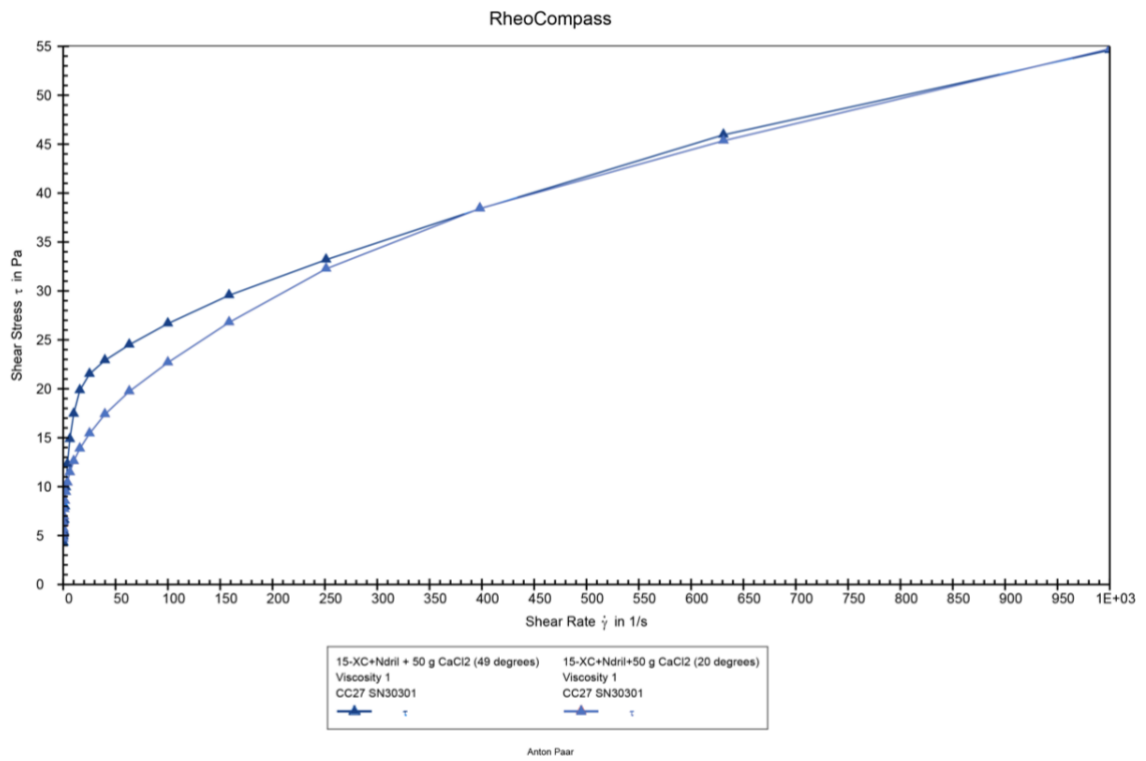
Figure 4.4.5: Flow curve of XC + Ndril + 50 g CaCl₂ (rheometer data)

4.5   Analysis of Herschel-Bulkley Parameters and Salt Effects

This section analyzes the differences and effects of salts on Herschel-Bulkley parameters. Table 4.7 lists the calculated Herschel-Bulkley parameters using data from the rheometer. Values in the first row is at 20 °C, the second row is at 49 °C for each sample.

Table 4.7: Calculated Herschel-Bulkley parameters using data from rheometer.

Sample	τ_y [Pa]	τ_s [Pa]	n
1-XC	4.73	1.93	0.6971
	4.43	2.09	0.6432
2-XC + PAC	9.17	9.32	0.7202
	5.52	5.87	0.7515
3-XC + PAC + 50 g NaCl	8.93	10.37	0.7276
	5.22	5.83	0.7765
4-XC + Ndril	10.41	3.81	0.7117
	7.98	3.17	0.6570
5- XC + Ndril + 50 g NaCl	10.67	5.38	0.6840
	7.96	3.92	0.6856
8-XC + Ndril + Auracoat	12.39	4.39	0.7126
	11.86	4.11	0.6306
11-XC + PAC + 50 g CaCl$_2$	9.71	5.46	0.7583
	8.51	3.71	0.8021
15-XC + Ndril + 50 g CaCl$_2$	14.41	8.44	0.6852
	21.63	5.15	0.8128

Table 4.8. shows the effects of salt on the Ndril solution. We observe that NaCl, CaCl$_2$ and Auracoat has a small effect on the curvature index at 20 °C. CaCl$_2$ increases n by 23 % at 49 °C. Opposite to the amplitude sweep the yield stress does not change for NaCl. This shows a limitation of calculating yield stress at higher shear rates. NaCl increases the surplus stress by 41 % at 20 °C. for 49 °C it increases by 24 %. Indicating that the effect of NaCl decreases at higher temperatures. Fluid 5 remains more thermostable than Fluid 4. This is observed for n with no change for Fluid 5 and a decrease of 7.7 % for Fluid 4.

Added CaCl$_2$ increases the parameters both at 20 °C and 49 °C. Showing that the stronger divalent Ca^{2+} ions have a large effect on the XC + Ndril solution. The increase in yield stress is 38 and 171 %. One could therefore argue that the shear stress increases more when reaching shear rates of 3 and 6 1/s compared to Fluid 4. Due to the higher surplus stress the viscosity increases more rapidly at increasing shear rates. A potential cause of the difference between CaCl$_2$ and NaCl. Could be that due to stronger reactions between Ca^{2+} ions and the hydrogen atoms in water. As well as CaCl$_2$'s higher solubility at higher temperatures, causing the viscosity to increase at higher temperatures.

Fluid with Auracoat shows a 19 and 15 % increase in yield and surplus stress. This could be because of the increased amount of particles and more bonding effects with the polymers.

However, more particles are not equivalent with increased viscosity (Sele, 2023). The change increases at 49 °C to 48 and 29 %. Because it is more thermostable than XC + Ndril where the parameters τ_y and τ_s decreased by 23 and 17 % respectively. With *n* remaining constant at 20 °C the shear thinning properties remains constant.

Table 4.8: Effects of different additives on 4-XC + Ndril. Presented as relative change in percent. First row is 20 °C, second is 49 °C for each sample.

Sample	τ_y [Pa]	τ_s [Pa]	*n*
3-XC + Ndril + 50 g NaCl	-2.50 %	-41.33 %	3.90 %
	0.20 %	-23.95 %	-4.35 %
15-XC + Ndril + 50 g CaCl$_2$	-38.36 %	-121.60 %	3.72 %
	-171.26 %	-62.66 %	-23.72 %
8-XC + Ndril + Auracoat	-19.00 %	-15.22 %	-0.13 %
	-48.72 %	-29.72 %	4.02 %

For XC + PAC, small changes in the curvature index were observed, like the observations for XC + Ndril. The effect of NaCl is 11% increased surplus stress at 20 °C. Otherwise the other parameters does not change by more than 5%. This shows that the monovalent Na$^+$ has a small impact on the Fluid 2. For XC + PAC + NaCl the yield stress decreases by 35 % with amplitude sweep measurements. As shown in Table 4.9 τ_y decreases by 2.7 %. It illustrates the difference between the two methods.

The effect of CaCl$_2$ is that the surplus stress decreases 42 % at 20 °C and 37 % at 49 °C, highlighting the effect of Ca^{2+} ions on the solution. One cannot conclude on whether XC, PAC or a combination of the two is most affected. But it is likely that it is a combination of both, as the effects are large and opposite to XC + Ndril. Note the difference in the yield stress when comparing the calculated with measured using amplitude sweep.

Table 4.9: : Effects of different additives on 2-XC + PAC. Presented as relative change in percent. First row is 20 °C, second is 49 °C for each sample.

Sample	τ_y [Pa]	τ_s [Pa]	*n*
3-XC + Pac + 50 g NaCl	2.68 %	-11.24 %	-1.03 %
	5.52 %	0.69 %	-3.33 %
11-XC + Pac + 50 g CaCl$_2$	-5.92 %	41.37 %	-5.29 %
	-54.19 %	36.84 %	-6.73 %

For both XC and Ndril the CaCl$_2$ have a larger effect compared to NaCl. The effect seems to be opposite for the surplus stress which decreases for Fluid 2 but increases for Fluid 4. A reason for this could be the difference between starch and cellulose polymer. Starch seems to form stronger bonds with XC preventing the Ca^{2+} ions to degrade the XC molecule. As both XC and PAC are anionic they repel each other leaving room for Ca^{2+} ions to bond with both XC and PAC. Therefore, increasing the degradation of the polymers and reducing their viscosifying effect.

4.6   Zeta Potential

The obtained results for the polymers diluted in the base fluid are listed in Table 4.10. As discussed in the theory section the fluid does not contain particles. Therefore, the obtained results should not be seen as concluding. However, we see that most of the theory matches the result because the fluids do have a pH in the range of 10-11. The results are related to the polymers behavior as if they were solid small particles.

Table 4.10: Measurements using zeta potential instrument for selected polymers.

Sample	Zeta potential (mV)	Standard deviation (mV)	Conductivity (mS/cm)
XC	-50.33	1.338	4.172
XC + PAC	-35.07	7.775	3.685
XC + Ndril HT	-21.62	3.743	2.261
XC + Dextrid E	-26.09	2.557	1.361
XC + Dextrid E + 50 g NaCl	2.053	3.697	162.2

The test using added NaCl also shows that the zeta potential drops. The practical usage of this is that it verifies that Na^+ ions forms bonds with the polymer. So that the electrical potential and attraction to other particles reduces. The fluid containing PAC also exhibits a higher absolute value. Indicating that it does not form equally strong bonds with the XC compared to the starch. The testing using base fluid shows the largest negative zeta potential, showing that xanthan gum forms a stable structure in water. See Figure 4.6.1 for a graphical representation of the results of fluids using XC, Ndril and PAC. 3 runs have been completed for each sample. One should take note that the fluids does not exhibit fully brownian motion and the obtained results should be inspected carefully.
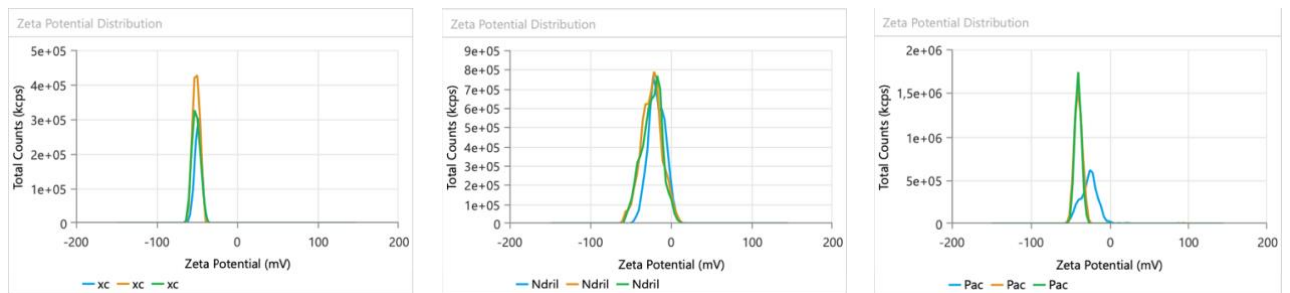
Figure 4.6.1: Graphical representation of Zeta potential measurements for selected samples.

5   Sources of Error

- Human error
    - The readings at the Ofite viscometer may be affected by human errors.
    - To ensure consistent results the procedures should be followed as described. Inconsistent ways of preparing fluids and readings will affect the results.
    - When dealing with high precision apparatus such as the rheometer, one is relying on a consequent procedure to avoid external errors.

- Equipment inaccuracy
    - The Ofite viscometer provide more stable readings at the higher range of high shear rates (100-600 RPM) and the measurements at lower shear rates from 3-100 the readings are more unstable the deviation of the viscometer was found to be 0.6 cP from Appendix D. This is calculated using the high shar rate measurements at 600 and 300 RPM. In addition, the viscometer does not have temperature control, and viscosity is very dependent on temperature. This is a benefit with the MCR 302 rheometer which offers highly stable temperature control.
    - Zeta potential measurements are originally a method for deciding the electrical potential at the slipping plane of particles. Polymers does not behave as particles. Thus, the reliability of the results can be discussed.

- Fluid properties
    - When xanthan gum solutions are mixed up at high shear rates, bubbles, and foam forms. Although these are removed AHR they are present in the measurements BHR. From experience the numbers BHR seems to be a bit higher than expected. More delicate mixing procedures over longer time and using lower shear rates allowing the XC to hydrate in the water should be considered in further research. This will also be gentler on the polymers.

To get a better view of the uncertainties when measuring viscosity using the concentric cylinder viscometer. Five samples of Fluid 1 are mixed and tested at the viscometer. From the obtained data as shown in Appendix C the uncertainty can be calculated. The calculated uncertainty for Fluid 1 has been done using the method described by Sele (2023) with Equations 5.1 and 5.2 below.

$$Uncertainty \; [\%] = \frac{standard \; deviation}{mean} * 100\% \qquad \textit{5.1}$$

$$Total \; standard \; deviation = \sqrt{\Sigma \sigma_i^2} \qquad \textit{5.2}$$

Table 5.1: Calculated uncertainties for 5 parallels of Fluid 1.

Rotational speed [1/s]	Mean deflection (θ)	Standard Deviation	Uncertainty
1022	14.1	0.306	2.166 %
510.9	10.5	0.298	2.831 %
340.6	9.2	0.161	1.757 %
170.3	7.6	0.191	2.511 %
102.2	6.6	0.161	2.433 %
51.09	5.9	0.161	2.750 %
10.22	4.4	0.204	4.598 %
5.11	4.0	0.102	2.532 %

6   Conclusion

Overall conclusions of this thesis can be summed up as:

- Adding NaCl and K_2SO_4 improves the fluids stability under thermal and mechanical wear. This applies to solutions using xanthan gum in combination with either PAC, Ndril HT and Dextrid E.
- Adding NaCl to XC + Ndril solutions resulted in a 41% increase in surplus stress at 20 °C. This effect was reduced at higher temperatures with a 24% increase at 49 °C.
- Adding $CaCl_2$ to XC + Ndril resulted in 38 and 171% increase in yield stress and surplus stress increased by 121 and 162% at 20 °C and 49 °C.
- Using $CaCl_2$ showed a destructive behavior on the XC + PAC solution. With a resulting 42 and 37 % reduction in surplus stress at 20 °C and 49 °C.
- The effect of hot rolling solutions of XC + PAC, XC + Ndril HT and XC + Dextrid E is a reduction of shear stress in the low shear rate range.
- The yield stress using amplitude sweeps decreased by 67 % for XC + Ndril using NaCl. The same was observed for added $CaCl_2$.
- For measurements of 49 °C the yield point of XC + Ndril did not increased with added salt.
- The rheometer provided more accurate measurements compared to the concentric cylinder viscometer. Especially in the important low shear rate region. Making the data better for comparison using the Herschel-Bulkley model.
- Results shows that xanthan gum forms stronger bonds with starches than cellulose polymers. This is confirmed from hot rolling tests, exposing the fluids to salts and zeta potential measurements.
- Auracoat UF increased the thermostability of XC + Ndril solutions. Adding Auracoat resulted in a 19 and 15 % increase in yield and surplus stress at 20 °C.
- XC + PAC showed increased thermostability for measurements at 49 °C in the LVE region compared to XC + Ndril. With yield stress decreasing 82 % from 20 °C to 49 °C. The equivalent for value XC + PAC was 48 %.
- Measurements conducted using zeta potential apparatus indicates that NaCl bonds with the polymers. This could be a reason why the stability increases.

7   References

Allouche, M.H., Botton, V., Henry, D., Millet, S., Usha, R., & Ben Hadid, H. (2014) Experimental determination of the viscosity at very low shear rate for shear thinning fluids by electrocapillarity. *Journal of Non-Newtonian Fluid Mechanics*, 215, 60-69. https://doi.org/10.1016/j.jnnfm.2014.11.003

AMC drilling optimisation. (2019). *AMC Salt Tables*. https://amcmud.com/wp-content/uploads/sites/2/2019/10/AMC-Salt-Tables-August2019.pdf (Approached 15.01.2024)

Anton Paar. (2024). *Amplitude sweeps*. Anton Paar wiki, https://wiki.anton-paar.com/en/amplitude-sweeps/ (Approached 10.04.2024)

Busch, A., Myrseth, V., Khatibi, M., Skjetne, P., Hovda, S., & Johansen, S. T. (2018). Rheological Characterization of Polyanionic Cellulose Solutions with Application to Drilling Fluids and Cuttings Transport Modeling. *Applied rheology, 28, 1-16*. http://doi.org/10.3933/ApplieRheol-28-25154

Chaturvedi, S., Kulshrestha, S., Bhardwaj, K., & Jangir, R. (2021). A Review on Properties and Applications of Xanthan Gum. *Microbial polymers*. Springer, Singapore: https://doi.org/10.1007/978-981-16-0045-6_4

Davoodi, S., Al-Shargabi, M., Wood, D., Rukavishnikov, V., & Minaev, K. (2024). Synthetic polymers: A review of applications in drilling fluids. *Petroleum Science*, 475-518.

Hossain, M. E., & Al-Majed, A. A. (2015). *Fundamentals of Sustainable Drilling Engineering (1st ed). WILEY*. https://doi.org/10.1002/9781119100300

Jadav, M., Pooja, D., Adams, D., & Kulhari, H. (2023). Advances in Xanthan Gum-Based Systems for the Delivery of Therapeutic Agents. *Pharmaceutics 15(2)*. https://doi.org/10.3390/pharmaceutics15020402

Klungtvedt, K. R., & Saasen, A. (2022a). Comparison of Lost Circulation Material Sealing Effectiveness in Water-Based and Oil-Based Drilling Fluids and Under Conditions of Mechanical Shear and High Differential Pressures. ASME. J *Energy Resour. Technol*. December 2022; 144(12): 123011. https://doi.org/10.1115/1.4054653

Klungtvedt, K. R., & Saasen, A. (2022b). Invasion of CaCO3 particles and polymers into porous formations in presence of fibres. *Journal of Petroleum Science and Engineering*, 215 (2022) 110614. https://doi.org/10.1016/j.petrol.2022.110614

Mateus, R. V., & Rosângela, B. Z. (2019). Concentration, Brine Salinity and Temperature effects on Xanthan Gum Solutions Rheology. *Applied Rheology*, 29, 69-79. https://doi.org/10.1515/arh-2019-0007

Mezger, T. G. (2015). *Applied rheology (2nd ed.)*. Anton Paar.

Mohammed, Z., Haque, A., Richardson, R., & Morris, E. (2007). Promotion and inhibition of xanthan 'weak-gel' rheology by calcium ions. *Carbohydrate polymers, 70(1)*, pp. 38-45. https://doi.org/10.1016/j.carbpol.2007.02.026

Nakajima, H., Dijkstra, P., & Loos, K. (2017). The Recent Developments in Biobased Polymers toward General and Engineering Applications: Polymers that Are Upgraded from Biodegradable Polymers, Analogous to Petroleum-Derived Polymers, and Newly Developed. *Polymers* 9(10). https://doi.org/10.3390/polym9100523

Nelson, A., & Ewoldt, R. (2017). Design of yield-stress fluids: a rheology-to-structure inverse problem. *Soft matter*, 13(41), 7578-7594. https://doi.org/10.1039/C7SM00758B

Nobbmann, U. (2018). Zeta potential in salt solution (or any other ions).*Malvern Panalytical*: https://www.materials-talks.com/zeta-potential-in-salt-solution-or-any-other-ions/ (Approached 12.03.2024)

Nsengiyumva , E. M., Heitz, M. P., & Alexandridis, P. (2023). Salt and Temperature Effects on Xanthan Gum Polysaccharide in Aqueous Solutions . *International Joournal of Molecular Sciences*, 25(1), 490. https://doi.org/10.3390/ijms25010490

Ofei, T. N., Ngoumba, E., Opedal, N., Lund, B., & Saaasen, A. (2023). Rheology assessment and barite sag in a typical North Sea oil-based drilling fluid at HPHT conditions. *Korea-Australia Rheology Journal*, 35, 81-94. https://doi.org/10.1007/s13367-023-00055-0

Power D & Zamora, M. (2003). Drilling Fluid Yield Stress: Measurement Techniques for Improved Understanding of Critical Drilling Fluid Parameters. Paper AADE-03-NTCE-35, AADE 2003 National Technology Conference , Houston.

Saasen, A., & Ytrehus, J. D. (2020, October 11). Viscosity Models for Drilling Fluids—Herschel-Bulkley Parameters and Their Use . *Energies, 13(20), 5271*. https://doi.org/10.3390/en13205271

Sele, K. (2023). *Lost Circulation Material Impact on Water-Based Drilling Fluids' Viscous Properties: Herschel-Bulkley Fluid Characterization using Dimensionless Shear Rates.* [Bacelor's thesis]. University of Stavanger.

Shashikant, K., Agrawal, S., Cherumukkil, S., Sharma, V., Jasra, R. V., & Munshi, P. (2022). Revisiting Zeta potential, the Key Feature of Interfacial Phenomena, with Applications and Recent Advancements. *Chemistry Select*, 7(1). https://doi.org/10.1002/slct.202103084

Wei, W., Wu, M., Zhang, T., Zhang, X., Ren, W., & He, T. (2023). Enhancement of Starch Gel Properties Using Ionic Synergistic Multiple Crosslinking Extrusion Modification. *Foods*, 13(1), 24. https://doi.org/10.3390/foods13010024

Wyatt Technology. (2024, March 25). Charge & Zeta Potential [illustration]. https://d6hjj6q0hwmhv.cloudfront.net/wp-content/uploads/2023/09/FIDELIS-Diagram-Final-1000.jpg (Approached: 10.04.2024)

8 Appendix A

Table 8.1 A-1: Recipe and mixing sequence for samples 1-8 in grams unless stated otherwise.

	1	2	3	4	5	6	7	8
Sample size [ml]	350	350	350	350	350	350	350	350
Water	348	341.2	326.5	338.2	323.6	339.3	324.7	327.3
Soda ash	0.02	0.02	0.02	0.02	0.02	0.02	0.02	0.02
Caustic Soda	0.25	0.25	0.25	0.25	0.25	0.25	0.25	0.25
XC (BARAZAN)	1.5	1.5	1.5	1.5	1.5	1.5	1.5	1.5
PAC-L		5.0	5.0					
Starch (N-DRIL HT)				5.0	5.0			5.0
Starch (Dextrid-E)						5.0	5.0	
MgO	1.0	1.0	1.0	1.0	1.0	1.0	1.0	1.0
CaCl2								
NaCl			50		50		50	
Auracoat								5.0
K2SO4								

Table 8.2 A-2: Recipe and mixing sequence for samples 9-16 in grams unless stated otherwise.

	9	10	11	12	13	14	15	16
Sample size [ml]	350	350	350	350	350	350	350	350
Water	332	332	332	334.8	334.8	334.2	328.9	315.8
Soda ash	0.02	0.02	0.02	0.02	0.02	0.02	0.02	0.02
Caustic Soda	0.25	0.25	0.25	0.25	0.25	0.25	0.25	0.25
XC (BARAZAN)	1.5	1.5	1.5	1.5	1.5	1.5	1.5	1.5
PAC-L			5.0	5.0				
Starch (N-DRIL HT)		5.0			5.0	5.0	5.0	5.0
Starch (Dextrid-E)	5.0							
MgO	1.0	1.0	1.0	1.0	1.0	1.0	1.0	1.0
CaCl2			50		2 5		50	100
NaCl	25	25						
Auracoat								
K2SO4				35		25		

9   Appendix B

List of equipment used in this thesis.

1) *OFITE 93-99 Model 800 8-Speed Viscometer*
   a) *Speed Accuracy [rpm]= 0,1*
   b) *R1B1 F1.0*
2) Thermometer Clas Ohlson article number 36-1833
   a) Range from -50 °C to 300 °C
   b) Accuracy of ±1 °C for temperatures between -30 °C to 250 °C
3) VWR Water-Resistant/Shock-Resistant and Waterproof/Shockproof Stopwatch.
   a) Accuracy: 0,01
4) Hamilton Beach Mixer
   a) Spindle speed high: 23,900 rpm
   b) Spindle speed medium: 21,800 rpm
   c) Spindle speed low: 16,300 rpm
5) Mettler Toledo PB1502-S/FACT
   a) Capacity of 1510g
   b) Readability of 0.01g
   c) Linearity of 0.02g
6) OFITE Roller Oven 172-00-1-RC
   a) Temperature Range: 100 - 450°F (38 - 232.2°C)
   b) Capable of maintaining a temperature of 150° F ± 5° F (65° C ± 3° C)
7) Threaded stainless steel rod used in Hot Rolling
   a) Provided by the Department of Mechanical and Structural Engineering and Materials Science at UiS
   b) Pitch: 2 mm
   c) Length: 140 mm
   d) Weight: 183.5 g
8) Zetasizer advanced series lab
   a) Size measurement principle: Classical 90° Dynamic Light Scattering
   b) Zeta Measurement principle: ELS with M3-PALS and Constant Current Zeta Mode
   c) Molecular Weight and B22 principle: Static Light Scattering (90°)
   d) Size range: 0.3 nm to 10 μm
   e) Zeta potential size range: 3.8 nm to 100 μm
9) Anton Paar MCR 302 rheometer
   a) Measurements done with fluid between cup and bob.

10 Appendix C

Table 10.1 C-1: 5 parallel measurements sequence for 1-XC.

	1	2	3	4	5
1021,8	14,2996	14,2996	13,7889	13,7889	14,55495
510,9	10,214	10,7247	10,46935	10,214	10,98005
340,6	9,1926	9,1926	9,1926	8,93725	9,44795
170,3	7,6605	7,6605	7,40515	7,40515	7,91585
102,18	6,6391	6,6391	6,6391	6,38375	6,89445
51,09	6,1284	5,87305	5,87305	5,6177	5,87305
10,218	4,5963	4,5963	4,34095	4,0856	4,5963
5,109	4,0856	4,0856	4,0856	3,83025	4,0856

11 Appendix D

Table 11.1 D-1: Ofite calibration fluid

OFITE
Dependable Products From People We Trust

11302 Steeplecrest Dr. Houston, Texas 77065 Phone 832-320-7300 Fax 713-880-9885 www.ofite.com

NIST CERTIFIED CALIBRATION FLUID, 100 cP
OFI Part No. 132-80
LOT NO. 202703, Sample ID: V5100, Issued: April 1, 2022

30.06.25

°C	cP	°C	cP	°C	cP	°C	cP	°C	cP
20.0	106.0	24.0	98.2	28.0	91.0	32.0	84.3	36.0	78.2
20.1	105.8	24.1	98.0	28.1	90.8	32.1	84.2	36.1	78.0
20.2	105.6	24.2	97.8	28.2	90.7	32.2	84.0	36.2	77.9
20.3	105.4	24.3	97.7	28.3	90.5	32.3	83.8	36.3	77.7
20.4	105.2	24.4	97.5	28.4	90.3	32.4	83.7	36.4	77.6
20.5	105.0	24.5	97.3	28.5	90.1	32.5	83.5	36.5	77.4
20.6	104.8	24.6	97.1	28.6	90.0	32.6	83.4	36.6	77.3
20.7	104.6	24.7	96.9	28.7	89.8	32.7	83.2	36.7	77.1
20.8	104.4	24.8	96.7	28.8	89.6	32.8	83.1	36.8	77.0
20.9	104.2	24.9	96.5	28.9	89.5	32.9	82.9	36.9	76.9
21.0	104.0	25.0	96.4	29.0	89.3	33.0	82.7	37.0	76.7
21.1	103.8	25.1	96.2	29.1	89.1	33.1	82.6	37.1	76.6
21.2	103.6	25.2	96.0	29.2	88.9	33.2	82.4	37.2	76.4
21.3	103.4	25.3	95.8	29.3	88.8	33.3	82.3	37.3	76.3
21.4	103.2	25.4	95.6	29.4	88.6	33.4	82.1	37.4	76.1
21.5	103.0	25.5	95.4	29.5	88.4	33.5	82.0	37.5	76.0
21.6	102.8	25.6	95.3	29.6	88.3	33.6	81.8	37.6	75.9
21.7	102.6	25.7	95.1	29.7	88.1	33.7	81.6	37.7	75.7
21.8	102.4	25.8	94.9	29.8	87.9	33.8	81.5	37.8	75.6
21.9	102.2	25.9	94.7	29.9	87.8	33.9	81.3	37.9	75.4
22.0	102.0	26.0	94.5	30.0	87.6	34.0	81.2	38.0	75.3
22.1	101.9	26.1	94.4	30.1	87.4	34.1	81.0	38.1	75.1
22.2	101.7	26.2	94.2	30.2	87.3	34.2	80.9	38.2	75.0
22.3	101.5	26.3	94.0	30.3	87.1	34.3	80.7	38.3	74.9
22.4	101.3	26.4	93.8	30.4	86.9	34.4	80.6	38.4	74.7
22.5	101.1	26.5	93.6	30.5	86.8	34.5	80.4	38.5	74.6
22.6	100.9	26.6	93.5	30.6	86.6	34.6	80.3	38.6	74.4
22.7	100.7	26.7	93.3	30.7	86.4	34.7	80.1	38.7	74.3
22.8	100.5	26.8	93.1	30.8	86.3	34.8	80.0	38.8	74.2
22.9	100.3	26.9	92.9	30.9	86.1	34.9	79.8	38.9	74.0
23.0	100.1	27.0	92.8	31.0	85.9	35.0	79.7	39.0	73.9
23.1	99.9	27.1	92.6	31.1	85.8	35.1	79.5	39.1	73.7
23.2	99.7	27.2	92.4	31.2	85.6	35.2	79.4	39.2	73.6
23.3	99.5	27.3	92.2	31.3	85.5	35.3	79.2	39.3	73.5
23.4	99.4	27.4	92.0	31.4	85.3	35.4	79.1	39.4	73.3
23.5	99.2	27.5	91.9	31.5	85.1	35.5	78.9	39.5	73.2
23.6	99.0	27.6	91.7	31.6	85.0	35.6	78.8	39.6	73.1
23.7	98.8	27.7	91.5	31.7	84.8	35.7	78.6	39.7	72.9
23.8	98.6	27.8	91.3	31.8	84.6	35.8	78.5	39.8	72.8
23.9	98.4	27.9	91.2	31.9	84.5	35.9	78.3	39.9	72.7

	A =	B =	C =	D =
For Temp(T)<40°C	-0.00024378	0.04443182	-3.71983489	165.45801865
For Temp(T)>40°C	-0.00004912	0.01772772	-2.44695879	144.60318274

Viscosity (cP) = $A(T)^3 + B(T)^2 + C(T) + D$ (T) is in °C

Calibration of viscometer - OFITE 93-99 Model 800 8-Speed

Date: 01.02.202
Performed by: Morten Rosland / Jorunn H. Vrålstad Place: 6
s/n: 93-99

VWR Water-Resistant/Shock-Resistant and Waterproof/Shockproof Stopwatch - Accuracy 0,01%

Temperature [°C]: 18.7

- Thermometer Clas Ohlson article number 36-1833

- - Range from -50 °C to 300 °C
- - Accuracy of ±1 °C for temperatures between -30 °C to 250 °C

  Speed Accuracy [rpm]= 0,1

- - Using calibration fluid: 100 cP (Ofite), Batch:202703 (used).

Measurements of components:

- Rotor Sleeve - R1:
- Rotor Radius: 1,8415 cm

- Rotor diameter: 3,683 cm

- Bob-B1
- Bob Radius: 1,7245 cm

- Bob diameter: 3,449 cm - Bob height: 3,8 cm

- Torsion Spring - F1.0

- - Shear Stress Constant for Effective Bob Surface k_s [m^3] = 0.01323
- - Overall Instrument Constant K= 300
- - Minimum Spring Factor (F) for R1B1= 1,0

Table 11.2 D-2: Calibration fluid measurements.

Model	Ofite Model 800, 8 speed
s/n	93-99
600	217
300	109
200	73
100	36.5
60	22
30	11
6	2
3	1
Calulated [cP]	108
Expected [cP]	108.6
Temp (°C)	18.7
Comment	Low temperature. Values under 20° C calculated using linear interpolation.

Table 11.2 D-2: Calibration fluid measurements.
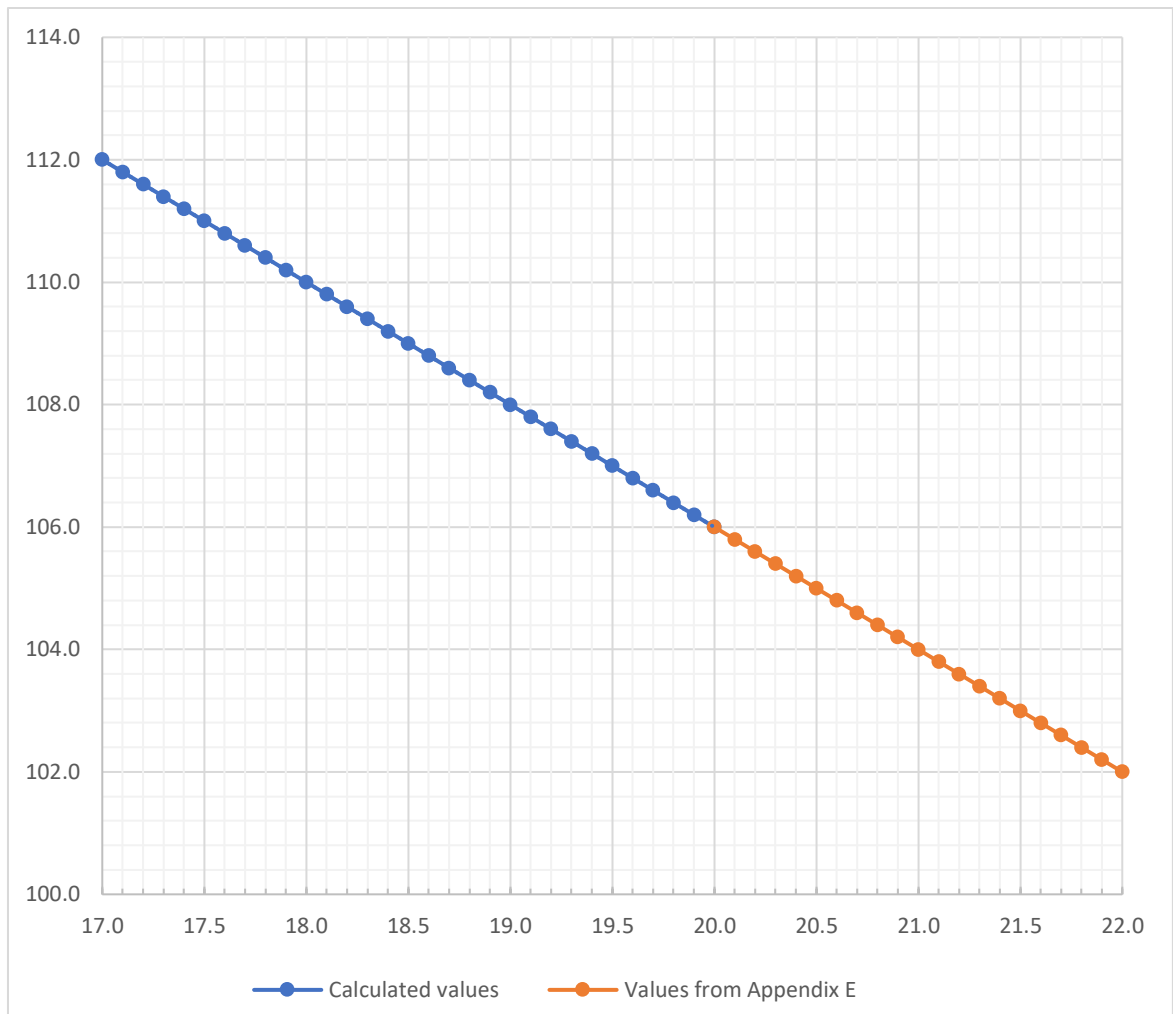
Figure 4.6.1 D-1: Calibration fluid, 100 cP (batch 202703)
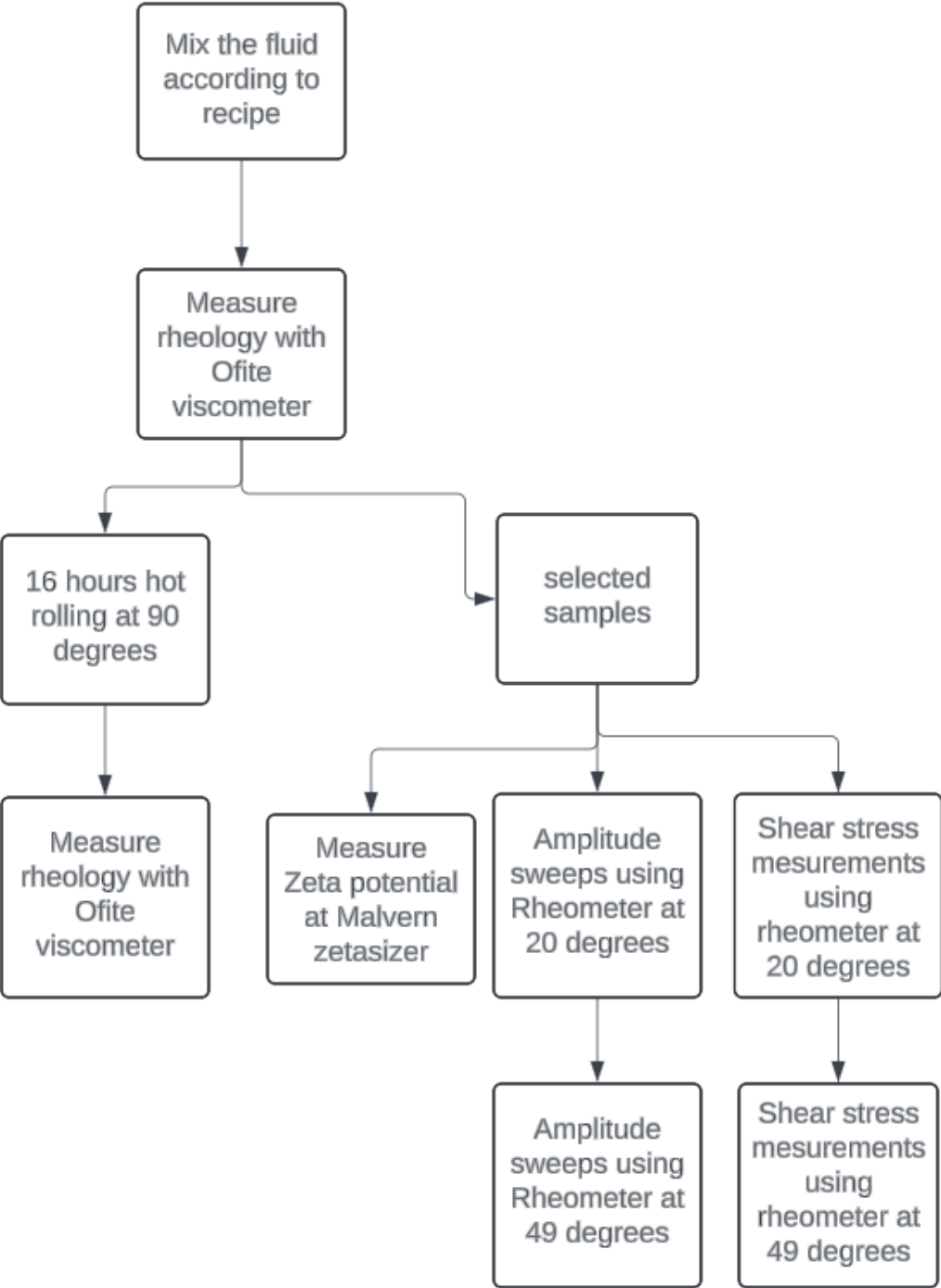
12 Appendix E

Figure 4.6.1 E-1: Procedure illustration.
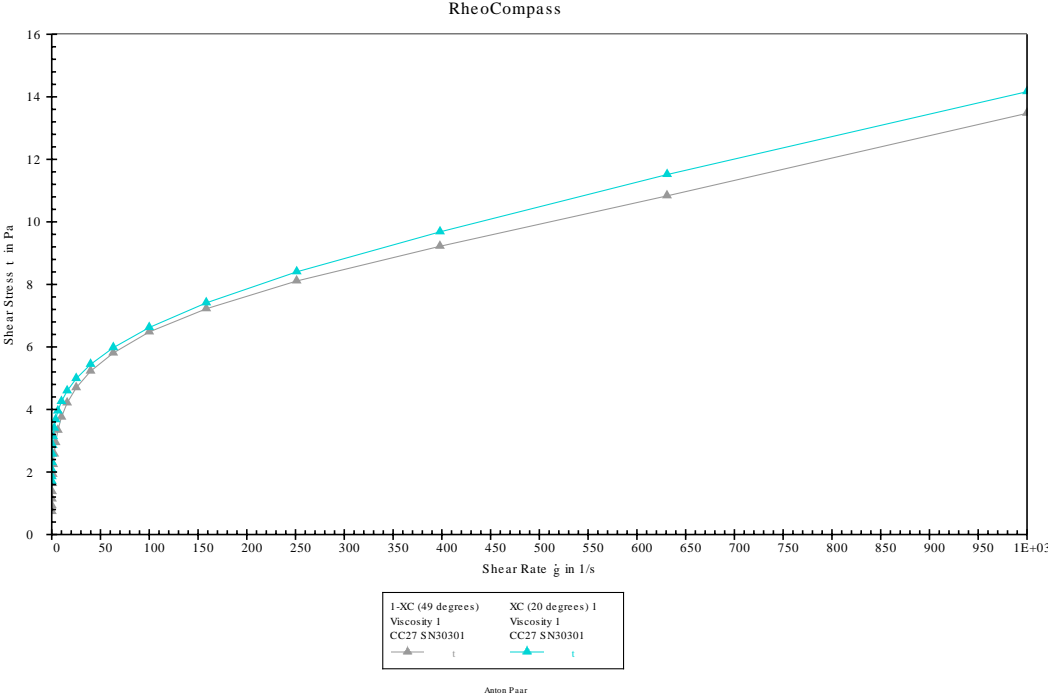
13 Appendix F
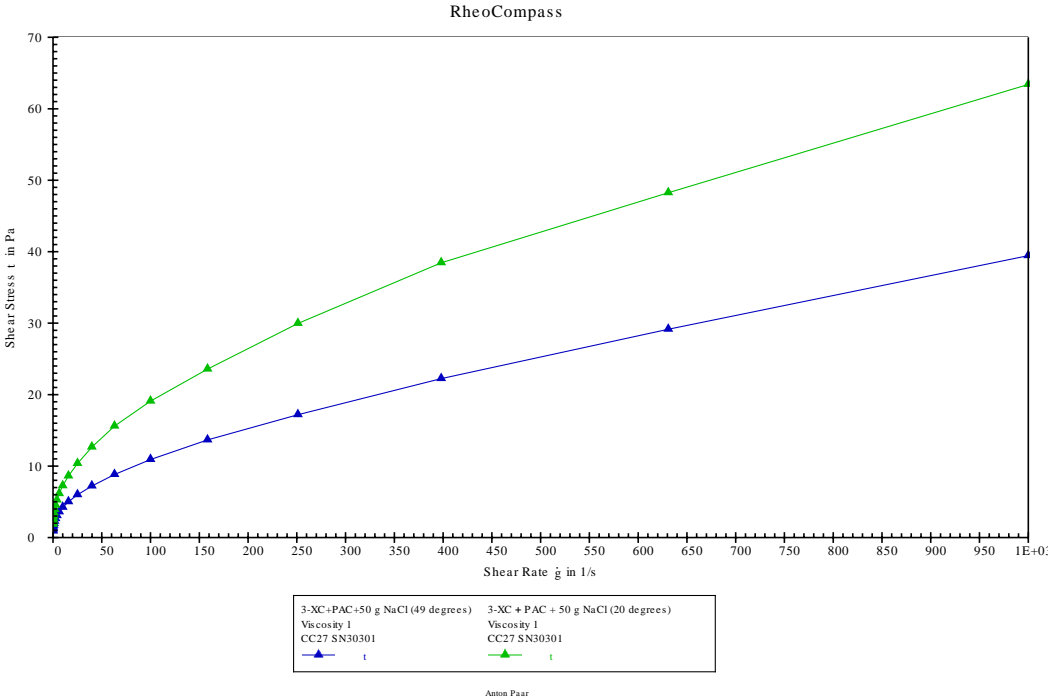

Figure 4.6.1 F-1: Flow curve of XC (rheometer data).

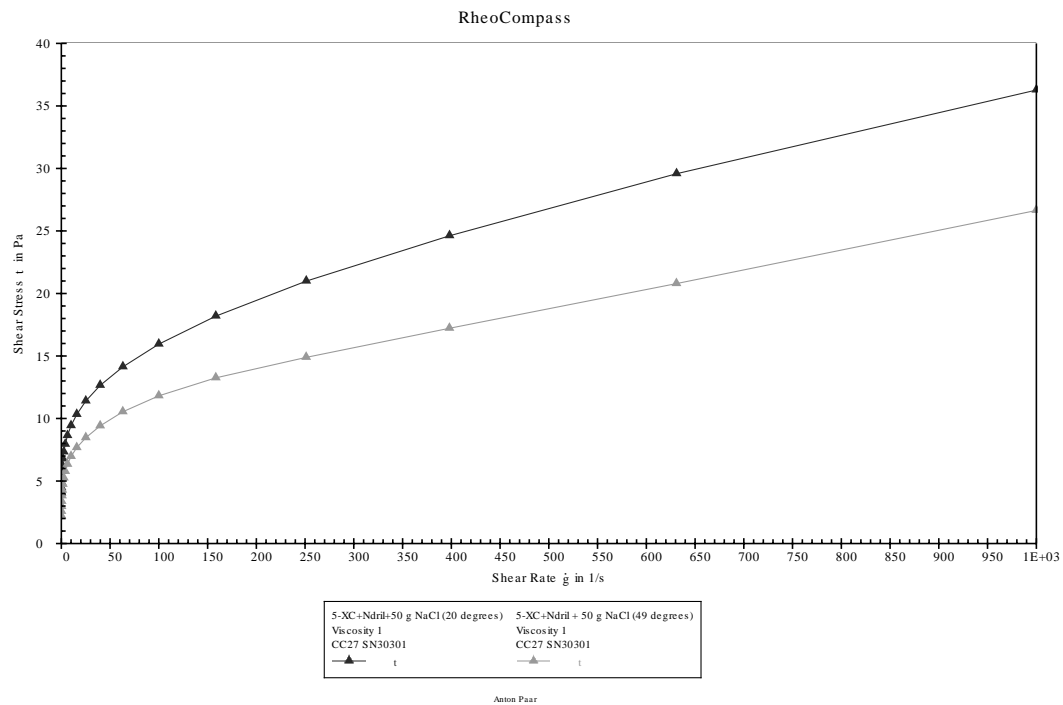*Figure 4.6.2 F-2: Flow curve of XC + PAC + 50 g NaCl (rheometer data).*

Figure 4.6.3 F-3: Flow curve of XC + Ndril + 50 g NaCl (rheometer data).

14 Appendix G

Python code used to calculate salt amount used in the different fluids.

```
"""
Created on Tue Jan 30 14:51:26 2024

@author: mortenrosland
"""

number_of_polymers = int(input('Number of chemicals added beside base recipe '))

def calculate_amount():
    # Constants for substances
    sodaash_mass = 0.02  # in grams
    sodaash_density = 2.54  # in g/cm^3

    caustic_soda_amount = 0.25
    caustic_soda_density = 2.13

    mgo_mass = 1
    mgo_density = 3.58

    xc_mass=1.5
    xc_density=0.839

    # Sample volume
    sample_volume = 350  # ml

    # Calculate substance amounts
    sodaash_amount = (sodaash_mass) / sodaash_density
    caustic_soda_amount = (caustic_soda_amount)/caustic_soda_density
    mgo_amount = (mgo_mass) / mgo_density
    xc_amount=(xc_mass)/xc_density

    # Print results for each substance
    print(f'Amount of sodaash: {sodaash_amount:.2f} ml')
    print(f'Amount of caustic soda: {caustic_soda_amount:.2f} ml')
    print(f'Amount of mgo: {mgo_amount:.2f} ml \n')

    remaining_volume = sample_volume - sodaash_amount - caustic_soda_amount - mgo_amount - xc_amount
    print(remaining_volume)

    #Add chemicals besides base recipe
    for i in range(number_of_polymers):
        polymer_mass = float(input(f'Enter mass for polymer {i + 1} (in grams): '))
        polymer_density = float(input(f'Enter density for polymer {i + 1} (in g/cm^3): '))
        polymer_amount = (polymer_mass) / polymer_density

        print(f'Amount of polymer {i + 1}: {polymer_amount:.2f} ml')

        # Update sample_volume for the remaining amount
        sample_volume -= polymer_amount

    # Print remaining amount
    #print(f'Remaining amount: {sample_volume:.2f} ml \n')

    return sample_volume
```

```python
def calculate_salt_water_amount():
    salt_amount_per_350ml = float(input('Enter the amount of salt per 350 ml (in grams): '))

    # Convert the salt amount to kg/m³
    salt_amount_kg_per_m3 = salt_amount_per_350ml * 1000 / 350

    print(f'Amount of salt per 350 ml: {salt_amount_per_350ml} grams')
    print(f'Amount of salt per m³: {salt_amount_kg_per_m3:.2f} kg/m³ \n')

    return salt_amount_kg_per_m3


def linear_interpolation(x1, y1, x2, y2, x):
    #Avoid division by zero
    if x1 == x2:
        raise ValueError("x1 and x2 cannot be equal")

    # Calculate the y-value using linear interpolation
    y = y1 + (y2 - y1) * (x - x1) / (x2 - x1)

    return y

# Specify the x-value to interpolate for
x = calculate_salt_water_amount()

# Specify the known points (x1, y1) and (x2, y2) from AMC tables
print("Table Values")
x1 = float(input("Enter x1 value "))
y1 = float(input("Enter y1 value "))
x2 = float(input("Enter x2 value "))
y2 = float(input("Enter y2 value "))

# Call the linear interpolation function
interpolated_y = linear_interpolation(x1, y1, x2, y2, x)

# Print the result
print(f"Interpolated y-value for x = {x}: {interpolated_y}")

water_volume = interpolated_y * calculate_amount()

print(water_volume)
```